Published by Institute of Physics Publishing for SISSA

Received: *November 15, 2007*
Revised: *December 21, 2007*
Accepted: *January 1, 2008*
Published: *January 17, 2008*

Heavy quarkonium in any channel in resummed hot QCD

Y. Burnier, M. Laine and M. Vepsäläinen

Faculty of Physics, University of Bielefeld,
D-33501 Bielefeld, Germany
E-mail: yburnier@physik.uni-bielefeld.de, laine@physik.uni-bielefeld.de, mtvepsal@physik.uni-bielefeld.de

Abstract: We elaborate on the fact that quarkonium in hot QCD should not be thought of as a stationary bound state in a temperature-dependent real potential, but as a short-lived transient, with an exponentially decaying wave function. The reason is the existence of an imaginary part in the pertinent static potential, signalling the "disappearance", due to inelastic scatterings with hard particles in the plasma, of the off-shell gluons that bind the quarks together. By solving the corresponding Schrödinger equation, we estimate numerically the near-threshold spectral functions in scalar, pseudoscalar, vector and axial vector channels, as a function of the temperature and of the heavy quark mass. In particular, we point out a subtlety in the determination of the scalar channel spectral function and, resolving it to the best of our understanding, suggest that at least in the bottomonium case, a resonance peak *can* be observed also in the scalar channel, even though it is strongly suppressed with respect to the peak in the vector channel. Finally, we plot the physical dilepton production rate, stressing that despite the eventual disappearance of the resonance peak from the corresponding spectral function, the quarkonium contribution to the dilepton rate becomes *more pronounced* with increasing temperature, because of the yield from free heavy quarks.

Keywords: Thermal Field Theory, NLO Computations, Heavy Quark Physics.

JHEP01(2008)043

Contents

JHEP01(2008)043

1. Introduction

Assuming the existence of a thermalized medium, with a temperature T, and of heavy quarks, with a mass $M \gg T$, there is a finite probability, given by the Boltzmann factor $\exp(-2M/T)$, that an on-shell quark and antiquark are generated through thermal fluctuations. They could then annihilate, creating an off-shell photon, which may escape from the thermal system, and subsequently decay into a dilepton pair (for instance, e^-e^+ or $\mu^-\mu^+$). The characteristics of the energy distribution of these pairs offer an indirect probe on the strongly interacting dynamics taking place within the thermalized system. As a concrete application, properties of lepton pairs can be observed in heavy ion collision experiments (see, e.g., refs. [1]), and may serve as an indication of whether a thermalized state with a temperature above the deconfinement transition was momentarily reached during the evolution [2].

Given that various properties of the quarkonium system can be understood in great detail at zero temperature [3], it could be assumed that describing quantitatively the heavy quark-antiquark system in a thermalized medium is a relatively simple task. After all, QCD is asymptotically free, so the effective coupling should decrease with the temperature, and ultimately confinement is lost as well. Somewhat surprisingly, this expectation appears to be overly optimistic. In fact, all standard approximation methods develop further systematic uncertainties at $T > 0$. For instance, direct lattice QCD reconstructions of the quarkonium *spectral function* [4 – 6], which is a quantity determining the dilepton production rate, develop the new problem that an analytic continuation is needed from data collected on a short Euclidean time interval, to the observable defined in Minkowskian spacetime. Another popular class of approaches, so-called potential models [7, 8], suffers from the proliferation of many independent non-perturbative definitions of a "static potential" which could be measured on the lattice [9, 10] and inserted into a Schrödinger equation. A recently introduced method, the determination of the corresponding observable in strongly coupled $\mathcal{N} = 4$ Super-Yang-Mills theory [11], also contains unknown systematic errors from the point of view of QCD, which cannot be reduced by increasing the temperature, because the QCD coupling soon becomes weak [12].

The method employed in this paper is resummed weak-coupling perturbation theory. It again suffers from novel difficulties at finite temperatures: curing infrared divergences necessitates carrying out complicated resummations [13, 14], and even though a weak-coupling expansion in the QCD coupling constant g can subsequently be defined, it has a strange structure, with relative corrections suppressed only by odd powers of g [15, 16], by logarithms like $g^n \ln(1/g)$ [17, 18], or by powers of g multiplied by non-perturbative coefficients [19]–[21]. Moreover, even if a number of coefficients were known, the convergence of the series could be slow [22] (see, however, refs. [23, 12]).

Given all these problems, a suitable practical approach at the present date might be to compute the quarkonium spectral function and the dilepton production rate with many different methods, possessing complementary systematic errors, and to look for a consistent pattern, which could then also represent the situation in QCD. It is in this spirit that the purpose of the present paper is to pursue the side of resummed perturbative computations.

The resummed perturbative approach to heavy quarkonium in hot QCD was initiated in refs. [24]–[26], of which the present paper is a direct continuation. In particular, we expand and improve on the analysis of ref. [25]. We consider, first of all, the same observable as in ref. [25] (quarkonium spectral function in the vector channel), but discuss more extensively the dependence of the result on the temperature and on the heavy quark mass. Second, we carry out a new analysis for the spectral function in the scalar channel. This turns out to require more advanced numerical techniques than those used in ref. [25]. We also relate the pseudoscalar and axial vector spectral functions to the vector and scalar spectral functions. Finally, we elaborate on the physics implications of the results in more detail than before, both conceptually, i.e. with regard to the picture they suggest for the quarkonium system in a deconfined environment, and from the practical point of view, i.e. with regard to the dilepton production rate.

JHEP01(2008)043

2. General framework

We start by specifying somewhat more quantitatively the main ideas and equations of the resummed perturbative approach. A detailed derivation follows in sections 3, 4, while a reader only interested in the numerical results could skip directly to section 5 after the present section.

Let $\hat{\psi}$ be a generic heavy quark field operator in the Heisenberg picture. The basic correlation function we consider is of the form

$$C_>^V(t;\mathbf{r},\mathbf{r}') \equiv \int \mathrm{d}^3\mathbf{x} \left\langle \hat{\bar{\psi}}\left(t,\mathbf{x}+\frac{\mathbf{r}}{2}\right)\gamma^\mu\, W\, \hat{\psi}\left(t,\mathbf{x}-\frac{\mathbf{r}}{2}\right)\;\; \hat{\bar{\psi}}\left(0,-\frac{\mathbf{r}'}{2}\right)\gamma_\mu\, W'\, \hat{\psi}\left(0,+\frac{\mathbf{r}'}{2}\right)\right\rangle , \quad (2.1)$$

where W, W' are Wilson lines connecting the adjacent operators, inserted in order to keep the Green's function gauge-invariant; the metric is $\eta_{\mu\nu} = \mathrm{diag}(+---)$; and the expectation value refers to $\langle\ldots\rangle \equiv \mathcal{Z}^{-1}\mathrm{Tr}\,[\exp(-\hat{H}/T)(\ldots)]$, where $\mathcal{Z}$ is the partition function, $\hat{H}$ is the QCD Hamiltonian, and T is the temperature. The superscript in $C_>^V$ refers to the vector channel; the subscript refers to the time-ordering in eq. (2.1). We also consider scalar, pseudoscalar and axial vector correlators below; their precise definitions are given in section 3.[1]

The significance of the Green's function in eq. (2.1) is that if we take the limit $\mathbf{r},\mathbf{r}' \to \mathbf{0}$, and subsequently Fourier transform with respect to the time t, then we obtain a function which is trivially related to the heavy quarkonium spectral function, $\rho^V(\omega)$, in the vector channel:

$$\rho^V(\omega) = \frac{1}{2}\left(1-e^{-\frac{\omega}{T}}\right)\int_{-\infty}^{\infty}\mathrm{d}t\, e^{i\omega t}\, C_>(t;\mathbf{0},\mathbf{0})\,. \quad (2.2)$$

This quantity is physically important, given that the production rate of $\mu^-\mu^+$ pairs (with a vanishing total spatial momentum $\mathbf{0} = \mathbf{q}_{\mu^-} + \mathbf{q}_{\mu^+}$ and a non-vanishing total energy $\omega = E_{\mu^-} + E_{\mu^+}$) from a system at a temperature T, is directly proportional to $\rho^V(\omega)$ [27]:

$$\frac{\mathrm{d}N_{\mu^-\mu^+}}{\mathrm{d}^4x\,\mathrm{d}^4Q} = \frac{2c^2e^4}{3(2\pi)^5\omega^2}\left(1+\frac{2m_\mu^2}{\omega^2}\right)\left(1-\frac{4m_\mu^2}{\omega^2}\right)^{\frac{1}{2}} n_{\mathrm{B}}(\omega)\left[-\rho^V(\omega)\right], \quad (2.3)$$

where we assumed $\omega \geq 2m_\mu$; e is the electromagnetic coupling; $c \in (\frac{2}{3}\,,-\frac{1}{3}\,)$ is the electric charge of the heavy quark; and $n_{\mathrm{B}}(\omega) \equiv 1/[\exp(\omega/T)-1]$ is the Bose distribution function.

Now, a systematic perturbative determination of the Green's function in eq. (2.1), and of the corresponding spectral function in eq. (2.2), is quite difficult for energies ω close to the quark-antiquark threshold, $\omega \sim 2M$. The reason is that in this regime infinitely many graphs, particularly so-called ladders, contribute at the same order. A further problem is that at finite temperatures, the rungs of the ladders, containing gluons, need to be dressed by thermal corrections.

A way to resum these infinitely many dressed contributions is not to compute the correlator of eq. (2.1) directly, but rather to find a partial differential equation satisfied

[1] In ref. [24], we set $\mathbf{r}' = \mathbf{0}$, and denoted the correlator by $\check{C}_>(t,\mathbf{r}) \equiv C_>^V(t;\mathbf{r},\mathbf{0})$. However, with certain channels, it will be advantageous to keep $\mathbf{r}' \neq \mathbf{0}$, because then the singularities from the static potential at $\mathbf{r} = \mathbf{0}$, and from the initial condition of the Schrödinger equation at $\mathbf{r} = \mathbf{r}'$, do not overlap.

JHEP01(2008)043

by this correlator, and then to solve this equation numerically. The partial differential equation in question is just the Schrödinger equation. Indeed, it is for the sake of being able to write a Schrödinger equation that we have introduced $\mathbf{r}, \mathbf{r}' \neq \mathbf{0}$ in eq. (2.1). To be more precise, let us consider $C_>^V$ in the limit that the heavy quark mass M is very large. Then, as we will see, $C_>^V$ obeys

$$\left\{ i\partial_t - \left[2M + V_>(t,r) - \frac{\nabla_{\mathbf{r}}^2}{M} + \mathcal{O}\left(\frac{1}{M^2}\right) \right] \right\} C_>^V(t;\mathbf{r},\mathbf{r}') = 0 \;, \tag{2.4}$$

with the initial condition

$$C_>^V(0;\mathbf{r},\mathbf{r}') = -6N_{\rm c}\,\delta^{(3)}(\mathbf{r}-\mathbf{r}') + \mathcal{O}\left(\frac{1}{M}\right) , \tag{2.5}$$

where $N_{\rm c} = 3$. The terms specified explicitly in eqs. (2.4), (2.5) result from a tree-level computation; in contrast, the potential denoted by $V_>(t,r)$ originates only at 1-loop order. It can be defined as the coefficient scaling as $\mathcal{O}(M^0)$, after acting on $C_>^V(t;\mathbf{r},\mathbf{r}')$ with the time derivative $i\partial_t$. The potential $V_>(t,r)$ depends, in general, on the temperature; we assume that T is parametrically low compared with the heavy quark mass, $T \sim (g^2 \ldots g)M$ (cf. section 3.1).

Now, it can be argued that in order to be parametrically consistent, the static potential in eq. (2.4) should be evaluated in the limit $t \gg r$ (cf. section 3.1). Then it obtains a simple form: in dimensional regularization (cf. eqs. (4.3), (4.4) of ref. [24]),

$$\lim_{t\to\infty} V_>(t,r) = -\frac{g^2 C_F}{4\pi}\left[m_{\rm D} + \frac{\exp(-m_{\rm D} r)}{r} \right] - \frac{i g^2 T C_F}{4\pi}\,\phi(m_{\rm D} r) + \mathcal{O}(g^4) \;, \tag{2.6}$$

where $C_F \equiv (N_{\rm c}^2 - 1)/2N_{\rm c}$; $m_{\rm D}$ is the Debye mass parameter; and the function

$$\phi(x) \equiv 2\int_0^\infty \frac{{\rm d}z\, z}{(z^2+1)^2}\left[1 - \frac{\sin(zx)}{zx} \right] \tag{2.7}$$

is finite and strictly increasing, with the limiting values $\phi(0) = 0$, $\phi(\infty) = 1$.

The first term in eq. (2.6) corresponds to twice a thermal mass correction for the heavy quarks (cf. the first term inside the square brackets in eq. (2.4)). The second term is a standard r-dependent Debye-screened potential. The third term represents an imaginary part: its physics is that almost static (off-shell) gluons may disappear due to inelastic scatterings with hard particles in the plasma. This is the phenomenon of Landau-damping, well-known in plasma physics. As a consequence of the imaginary part, the solution of the Schrödinger equation does not lead to a stationary wave function: rather, the bound state decays exponentially with time, representing a short-lived transient.

In the following two sections, we discuss the origin of the formulae presented here, and their practical evaluation, in some more detail. We also extend the discussion to the other channels. We return to the numerical solution of the Schrödinger equation in section 5.

3. Schrödinger equation and initial conditions

Our strategy for the derivation of the Schrödinger equation satisfied by the two-point correlation functions in various channels will be quite straightforward and "modest" here[2]: we

[2] A more systematic approach might follow by generalizing the framework of PNRQCD [28] to finite T.

first compute the correlation functions in tree-level perturbation theory, and then expand in inverse powers of the heavy-quark mass. At this point we can identify the Schrödinger-equation and the initial condition for its solution. Subsequently, radiative corrections are expected to multiplicatively correct the terms that already appear at tree-level, and to add other terms which are allowed by symmetries, even if they would not appear at tree-level; the most important of these is the static potential. As long as there is a hierarchy between the different physical scales relevant for the problem (cf. section 3.1), and we are only sensitive to perturbative scales, general principles suggest that the system should remain local in the presence of radiative corrections, and that a truncation to a certain order is possible.

3.1 Power counting

Let us consider the parametric orders of magnitude of the various terms in eq. (2.4), given the potential in eq. (2.6). We recall, first of all, that the term $2M$ plays no role, since it can always be eliminated through a trivial phase factor (cf. eq. (4.1)). Around the quarkonium peak, the time derivative (or energy) is then of the order of the kinetic terms, i.e. $\partial_t \sim \partial_r^2/M$. If we, furthermore, equate kinetic energy with the Coulomb potential energy (assuming $m_{\rm D} r \lesssim 1$, cf. below), we are lead to

$$\partial_r \sim \frac{1}{r} \sim g^2 M \;, \quad \partial_t \sim \frac{1}{t} \sim g^4 M \;. \tag{3.1}$$

An essential question is now to decide how the temperature, T, is to be compared with these scales. Let us assume, first of all, that

$$T \sim g^2 M \qquad \text{(case 1)} \;. \tag{3.2}$$

Then $m_{\rm D} r \sim g T r \sim g \ll 1$, and Debye screening plays essentially no role yet: we may assume the bound state to exist. In this limit,

$$\mathrm{Re}\, V_> \sim \frac{g^2}{r} \sim g^4 M \;\gg\; \mathrm{Im}\, V_> \sim g^2 T (m_{\rm D} r)^2 \sim g^6 M \;, \tag{3.3}$$

and the imaginary part can indeed be neglected.

On the other hand, let us increase the temperature to

$$T \sim g M \qquad \text{(case 2)} \;. \tag{3.4}$$

Then Debye screening plays an essential role, $m_{\rm D} r \sim g T r \sim 1$, and we may assume that the bound state has melted: indeed, in this limit,

$$\mathrm{Re}\, V_> \sim \frac{g^2}{r} \sim g^4 M \;\ll\; \mathrm{Im}\, V_> \sim g^2 T \sim g^3 M \;, \tag{3.5}$$

so that the imaginary part of the potential, or the width of the state, dominates over the real part of the potential, or the binding energy.

To summarise, the interesting temperature range is $T \sim (g^2 \ldots g) M$. In principle, parametrically consistent analyses in the two limiting cases may require different methods.

In practice, we would like to have phenomenological access to the whole range; therefore, in the present paper we work (implicitly) in the situation where $\mathrm{Re}\, V_> \sim \mathrm{Im}\, V_>$, setting us somewhere in the middle of the range. For further reference, let us point out that in this situation, $r\nabla A \sim r m_{\rm D} A \lesssim A$, where A is some gauge field component: the variation of the infrared gauge fields is parametrically small on the length scales set by the bound state radius.

3.2 Vector channel

Denoting

$$V^\mu(x;\mathbf{r}) \equiv \bar\psi\biggl(t,\mathbf{x}+\frac{\mathbf{r}}{2}\biggr)\gamma^\mu\, W\psi\biggl(t,\mathbf{x}-\frac{\mathbf{r}}{2}\biggr)\,, \tag{3.6}$$

where $x\equiv(t,\mathbf{x})$, the vector channel correlator we consider is in general of the type

$$C^V_>(x;\mathbf{r},\mathbf{r}') = \Bigl\langle V^\mu(x;\mathbf{r}) V_\mu(0;-\mathbf{r}')\Bigr\rangle\,. \tag{3.7}$$

For simplicity, we have left out hats from the fields in eq. (3.6), as is appropriate once we go over to the path integral formulation in Euclidean spacetime.

Now, even though we will carry out the computation of eq. (3.7) within QCD below, it will be useful to rewrite the operators considered in the language of NRQCD [29] (for a review, see ref. [30]), because this allows to immediately see their scaling with the heavy quark mass M, and because this allows to relate various operators to each other in the large-M limit. Following ref. [31], we can start by carrying out a Foldy-Wouthuysen transformation,

$$\psi \longrightarrow \exp\biggl(\frac{i\gamma^j\overrightarrow{D_j}}{2M}\biggr)\psi\,, \quad \bar\psi \longrightarrow \bar\psi\exp\biggl(-\frac{i\gamma^j\overleftarrow{D_j}}{2M}\biggr)\,, \tag{3.8}$$

where $\overrightarrow{D_j}\equiv\overrightarrow{\partial_j}-igA_j$, $\overleftarrow{D_j}\equiv\overleftarrow{\partial_j}+igA_j$, and we assume a summation over spatial indices, $j=1,2,3$. Afterwards, we go over to the non-relativistic two-component notation by writing

$$\psi\equiv\begin{pmatrix}\theta\\ \phi\end{pmatrix}\,, \quad \bar\psi\equiv(\theta^\dagger\,,\,-\phi^\dagger)\,, \tag{3.9}$$

where we already assumed a representation for the Dirac matrices with

$$\gamma^0\equiv\begin{pmatrix}\mathbb{1} & 0\\ 0 & -\mathbb{1}\end{pmatrix}\,, \quad \gamma^k\equiv\begin{pmatrix}0 & \sigma_k\\ -\sigma_k & 0\end{pmatrix}\,, \quad k=1,2,3\,. \tag{3.10}$$

Here σ_k are the Pauli matrices. Furthermore, it is useful to note that in NRQCD, the actions for ϕ and θ are of first order in time derivatives; consequently, one of the degrees of freedom propagates strictly forward in time, the other strictly backward in time, and a non-zero mesonic correlator at $t\neq 0$ is only obtained from structures like $\langle\phi^\dagger(\ldots)\theta\,\theta^\dagger(\ldots)\phi\rangle$.

We now find that for V^0, the leading term with the desired structure is $\mathcal{O}(1/M)$ (this term is also a total derivative in the limit $\mathbf{r}\to\mathbf{0}$). Therefore, the correlator $C^V_>$ is dominated by the spatial components V^k. At $\mathcal{O}(M^0)$, these become

$$V^k(x;\mathbf{r}) = \theta^\dagger\biggl(t,\mathbf{x}+\frac{\mathbf{r}}{2}\biggr)\sigma_k\, W\phi\biggl(t,\mathbf{x}-\frac{\mathbf{r}}{2}\biggr) + \phi^\dagger\biggl(t,\mathbf{x}+\frac{\mathbf{r}}{2}\biggr)\sigma_k\, W\theta\biggl(t,\mathbf{x}-\frac{\mathbf{r}}{2}\biggr)\,. \tag{3.11}$$

To the extent that interactions between the quark and antiquark are spin-independent (this is violated only at $\mathcal{O}(1/M)$), the Pauli-matrices play a trivial role in the two-point correlator made out of these operators, yielding eventually $\mathrm{Tr}\,[\sigma_k\sigma_l]$, if V^k and V^l are being correlated.

We now proceed to compute the correlator in eq. (3.7) at tree-level. We start in Euclidean spacetime[3] and after a spatial Fourier transform (for the moment we keep, for generality, the spatial momentum non-zero, $\mathbf{q}\neq\mathbf{0}$, unlike in eq. (2.1)), whereby

$$
\begin{aligned}
&C_E^V(\tau,\mathbf{q};\mathbf{r},\mathbf{r}') \\
&\equiv \int \mathrm{d}^3\mathbf{x}\, e^{-i\mathbf{q}\cdot\mathbf{x}}\left\langle \bar\psi\left(\tau,\mathbf{x}+\frac{\mathbf{r}}{2}\right)\gamma^\mu\,\psi\left(\tau,\mathbf{x}-\frac{\mathbf{r}}{2}\right)\;\bar\psi\left(0,-\frac{\mathbf{r}'}{2}\right)\gamma_\mu\psi\left(0,+\frac{\mathbf{r}'}{2}\right)\right\rangle \qquad (3.12)\\
&=-N_{\mathrm{c}}\int \mathrm{d}^3\mathbf{x}\, e^{-i\mathbf{q}\cdot\mathbf{x}}\sum\!\!\!\!\!\!\int_{\tilde P_{\mathrm{f}},\tilde S_{\mathrm{f}}} e^{i(\tilde p_{0\mathrm{f}}-\tilde s_{0\mathrm{f}})\tau+i(\mathbf{s}-\mathbf{p})\cdot\mathbf{x}+i(\mathbf{s}+\mathbf{p})\cdot\frac{\mathbf{r}-\mathbf{r}'}{2}}\,\mathrm{Tr}\left[\tilde\gamma_\mu\frac{-i\tilde{\not P}+M}{\tilde P^2+M^2}\tilde\gamma_\mu\frac{-i\tilde{\not S}+M}{\tilde S^2+M^2}\right]\\
&=-8N_{\mathrm{c}}\sum\!\!\!\!\!\!\int_{\tilde P_{\mathrm{f}},\tilde S_{\mathrm{f}}}(2\pi)^3\delta^{(3)}(\mathbf{s}-\mathbf{p}-\mathbf{q})e^{i(\tilde p_{0\mathrm{f}}-\tilde s_{0\mathrm{f}})\tau+i(2\mathbf{p}+\mathbf{q})\cdot\frac{\mathbf{r}-\mathbf{r}'}{2}}\;\frac{\tilde p_{0\mathrm{f}}\tilde s_{0\mathrm{f}}+\mathbf{p}\cdot\mathbf{s}+2M^2}{(\tilde P^2+M^2)(\tilde S^2+M^2)}\\
&=-4N_{\mathrm{c}}T^2\sum_{\tilde p_{0\mathrm{f}},\tilde s_{0\mathrm{f}}}\int\frac{\mathrm{d}^3\mathbf{p}}{(2\pi)^3}e^{i(\tilde p_{0\mathrm{f}}-\tilde s_{0\mathrm{f}})\tau+i(2\mathbf{p}+\mathbf{q})\cdot\frac{\mathbf{r}-\mathbf{r}'}{2}}\;\frac{2\tilde p_{0\mathrm{f}}\tilde s_{0\mathrm{f}}+E_{\mathbf{p}}^2+E_{\mathbf{p}+\mathbf{q}}^2+2M^2-\mathbf{q}^2}{(\tilde p_{0\mathrm{f}}^2+E_{\mathbf{p}}^2)(\tilde s_{0\mathrm{f}}^2+E_{\mathbf{p}+\mathbf{q}}^2)}\,,
\end{aligned}
$$

where $\tilde p_{0\mathrm{f}}=2\pi T(n+\frac{1}{2})-i\mu$, $n\in\mathbb{Z}$, denotes fermionic Matsubara frequencies (μ is the quark chemical potential), and we have introduced the notation

$$
E_{\mathbf{p}}\equiv\sqrt{M^2+\mathbf{p}^2}\,. \qquad (3.13)
$$

The Matsubara sums can be carried out, by making use of

$$
T\sum_{\tilde p_{0\mathrm{f}}}\frac{e^{\pm i\tilde p_{0\mathrm{f}}\tau}}{\tilde p_{0\mathrm{f}}^2+E^2}=\frac{1}{2E}\left[n_{\mathrm{F}}(E\pm\mu)e^{(\beta-\tau)E\pm\beta\mu}-n_{\mathrm{F}}(E\mp\mu)e^{\tau E}\right], \qquad (3.14)
$$

$$
T\sum_{\tilde p_{0\mathrm{f}}}\frac{\pm i\tilde p_{0\mathrm{f}}e^{\pm i\tilde p_{0\mathrm{f}}\tau}}{\tilde p_{0\mathrm{f}}^2+E^2}=-\frac{1}{2}\left[n_{\mathrm{F}}(E\pm\mu)e^{(\beta-\tau)E\pm\beta\mu}+n_{\mathrm{F}}(E\mp\mu)e^{\tau E}\right], \qquad (3.15)
$$

valid for $0<\tau<\beta$. This yields

$$
\begin{aligned}
C_E^V(\tau,\mathbf{q};\mathbf{r},\mathbf{r}')=&-N_{\mathrm{c}}\int\frac{\mathrm{d}^3\mathbf{p}}{(2\pi)^3}e^{i(\mathbf{2p}+\mathbf{q})\cdot\frac{\mathbf{r}-\mathbf{r}'}{2}}\times\\
&\times\Bigg\{n_{\mathrm{F}}(E_{\mathbf{p}}+\mu)n_{\mathrm{F}}(E_{\mathbf{p}+\mathbf{q}}-\mu)e^{(\beta-\tau)(E_{\mathbf{p}}+E_{\mathbf{p}+\mathbf{q}})}\left[\frac{-\mathbf{q}^2+2M^2+(E_{\mathbf{p}}+E_{\mathbf{p}+\mathbf{q}})^2}{E_{\mathbf{p}}E_{\mathbf{p}+\mathbf{q}}}\right]+\\
&+n_{\mathrm{F}}(E_{\mathbf{p}}+\mu)n_{\mathrm{F}}(E_{\mathbf{p}+\mathbf{q}}+\mu)e^{(\beta-\tau)E_{\mathbf{p}}+\tau E_{\mathbf{p}+\mathbf{q}}+\beta\mu}\left[\frac{\mathbf{q}^2-2M^2-(E_{\mathbf{p}}-E_{\mathbf{p}+\mathbf{q}})^2}{E_{\mathbf{p}}E_{\mathbf{p}+\mathbf{q}}}\right]+
\end{aligned}
$$

[3]Since both Euclidean and Minkowskian objects appear in this paper, we try to distinguish between them by denoting the former with a tilde. In particular, $\tilde P=(\tilde p_{0\mathrm{f}},\mathbf{p})$ denotes fermionic Euclidean four-momenta, while $\tilde\gamma_\mu$ stand for Euclidean Dirac matrices, satisfying $\{\tilde\gamma_\mu,\tilde\gamma_\nu\}=2\delta_{\mu\nu}$. Any further unspecified conventions can be found in ref. [24].

JHEP01(2008)043

$$+n_{\rm F}(E_{\mathbf{p}}-\mu)n_{\rm F}(E_{\mathbf{p+q}}-\mu)e^{(\beta-\tau)E_{\mathbf{p+q}}+\tau E_{\mathbf{p}}-\beta\mu}\left[\frac{\mathbf{q}^2-2M^2-(E_{\mathbf{p}}-E_{\mathbf{p+q}})^2}{E_{\mathbf{p}}E_{\mathbf{p+q}}}\right]+$$
$$+n_{\rm F}(E_{\mathbf{p}}-\mu)n_{\rm F}(E_{\mathbf{p+q}}+\mu)e^{\tau(E_{\mathbf{p}}+E_{\mathbf{p+q}})}\left[\frac{-\mathbf{q}^2+2M^2+(E_{\mathbf{p}}+E_{\mathbf{p+q}})^2}{E_{\mathbf{p}}E_{\mathbf{p+q}}}\right]\Bigg\}\,. \tag{3.16}$$

In order to simplify the expression somewhat, we note that once we go over into the spectral function[4], and restrict to frequencies (energies) around the quark-antiquark threshold, $|\omega-2M|\ll M$, then only the first of the structures in eq. (3.16) contributes. Second, close enough to the threshold, the δ-function expressing energy-conservation, $\delta(\omega-E_{\mathbf{p}}-E_{\mathbf{p+q}})$, forces the loop momentum $\mathbf{p}$ to be small, $|\mathbf{p}|\ll M$. We also assume the external momentum to be small, $|\mathbf{q}|\ll M$. Under these circumstances, we can expand

$$E_{\mathbf{p}}\approx M+\frac{\mathbf{p}^2}{2M}\,,\quad E_{\mathbf{p+q}}\approx M+\frac{|\mathbf{p}+\mathbf{q}|^2}{2M}\,, \tag{3.17}$$

and the relevant part of $C_E^V(\tau,\mathbf{q};\mathbf{r},\mathbf{r}')$ becomes

$$C_E^V(\tau,\mathbf{q};\mathbf{r},\mathbf{r}')$$
$$\simeq -6N_{\rm c}\int\frac{{\rm d}^3\mathbf{p}}{(2\pi)^3}e^{i(2\mathbf{p}+\mathbf{q})\cdot\frac{\mathbf{r}-\mathbf{r}'}{2}-\tau\left[2M+\frac{2\mathbf{p}^2+2\mathbf{p}\cdot\mathbf{q}+\mathbf{q}^2}{2M}+\mathcal{O}\left(\frac{1}{M^3}\right)\right]}\left[1+\mathcal{O}\left(\frac{1}{M^2}\right)\right]\,. \tag{3.18}$$

Here we have also omitted effects of relative order $\exp(-[M\pm\mu]/T)$, by keeping only the leading terms in the exponentials. We note that after these simplifications, all dependence on the temperature and on the chemical potential has disappeared from the tree-level result.

The real-time object we are ultimately interested in, is the analytic continuation

$$C_>^V(t,\mathbf{q};\mathbf{r},\mathbf{r}')=C_E^V(it,\mathbf{q};\mathbf{r},\mathbf{r}')\,. \tag{3.19}$$

Noting from eq. (3.18) that

$$-i\nabla_{\mathbf{r}}\Leftrightarrow\mathbf{p}+\frac{\mathbf{q}}{2}\,, \tag{3.20}$$

the dependence on $\mathbf{r}$ and t in the exponential amounts to satisfying the Schrödinger equation

$$\left\{i\partial_t-\left[2M+\frac{\mathbf{q}^2}{4M}-\frac{\nabla_{\mathbf{r}}^2}{M}+\mathcal{O}\left(\frac{1}{M^3}\right)\right]\right\}C_>^V(t,\mathbf{q};\mathbf{r},\mathbf{r}')=0\,. \tag{3.21}$$

The initial condition for the solution is obtained by setting $t=0$ in eq. (3.18) (after use of eq. (3.19)): we find

$$\begin{aligned}C_>^V(0,\mathbf{q};\mathbf{r},\mathbf{r}')&=-6N_{\rm c}\int\frac{{\rm d}^3\mathbf{p}}{(2\pi)^3}e^{i(2\mathbf{p}+\mathbf{q})\cdot\frac{\mathbf{r}-\mathbf{r}'}{2}}+\mathcal{O}\left(\frac{1}{M^2}\right)\\&=-6N_{\rm c}\,\delta^{(3)}(\mathbf{r}-\mathbf{r}')+\mathcal{O}\left(\frac{1}{M^2}\right)\,.\end{aligned} \tag{3.22}$$

[4]Take first a Fourier transform, $\tilde{C}_E(\omega_{\rm b})=\int_0^\beta{\rm d}\tau\,e^{i\omega_{\rm b}\tau}C_E(\tau)$, where $\omega_{\rm b}$ is a bosonic Matsubara frequency; then carry out the analytic continuation $\rho(\omega)=\frac{1}{2i}[\tilde{C}_E(-i[\omega+i0^+])-\tilde{C}_E(-i[\omega-i0^+])]$. A typical term in $C_E(\tau)$, of the form $\exp(\Delta_1\tau+\Delta_2(\beta-\tau))$, becomes $\rho(\omega)=-\pi(e^{\beta\Delta_1}-e^{\beta\Delta_2})\delta(\omega+\Delta_1-\Delta_2)$.

Eqs. (3.21), (3.22) justify eqs. (2.4), (2.5) for the vector channel in the free limit.

For future reference, let us also compute $\rho^V(\omega)$ explicitly (general expressions for free spectral functions can be found in refs. [38]). Eq. (3.18) (after $\tau \to it$) already shows the solution of eqs. (3.21), (3.22), and we can then directly remove the point-splitting, setting $\mathbf{r}, \mathbf{r}' = \mathbf{0}$. Shifting $\mathbf{p} \to \mathbf{p} - \mathbf{q}/2$; taking the steps in footnote 4; and ignoring exponentially small terms and terms suppressed by $\mathcal{O}(1/M^2)$, we find

$$\rho^V(\omega) \approx -6N_c\pi \int \frac{\mathrm{d}^3\mathbf{p}}{(2\pi)^3}\delta\biggl(\omega' - \frac{\mathbf{p}^2}{M}\biggr) = -\frac{3N_c}{2\pi}\,\theta(\omega')\,M^{\frac{3}{2}}\,(\omega')^{\frac{1}{2}} \;, \tag{3.23}$$

where

$$\omega' \equiv \omega - \biggl[2M + \frac{\mathbf{q}^2}{4M}\biggr] \,. \tag{3.24}$$

In the following, we will often for simplicity restrict to $\mathbf{q} = \mathbf{0}$ (like already in eq. (2.4)), but we can now observe from eqs. (3.23), (3.24) that the main effect of a non-zero $\mathbf{q} \neq \mathbf{0}$ is simply to shift the threshold location $2M$ by the center-of-mass kinetic energy $\mathbf{q}^2/4M$.

The analysis so far has been at tree-level. As argued in refs. [24, 25], however, the essential (temperature and ω-dependent) 1-loop corrections can be taken into account simply by inserting the potential $V_>(\infty, r)$, given in eq. (2.6), into eq. (3.21). There are of course also other loop corrections, related for instance to the renormalization and definition of M as a pole mass, and the overall normalization of the non-relativistic vector current in eq. (3.11); these corrections are in fact known to high order at zero temperature [32, 33],[5] but are not essential at our current resolution, so we mostly omit them here.

3.3 Scalar channel

Denoting

$$S(x;\mathbf{r}) \equiv \bar\psi\biggl(t, \mathbf{x} + \frac{\mathbf{r}}{2}\biggr) W \psi\biggl(t, \mathbf{x} - \frac{\mathbf{r}}{2}\biggr) \,, \tag{3.25}$$

the scalar channel correlator we consider is of the type

$$C^S_>(x;\mathbf{r},\mathbf{r}') = \Big\langle S(x;\mathbf{r}) S(0;-\mathbf{r}') \Big\rangle \,. \tag{3.26}$$

The correlator $C^S_>(x;\mathbf{0},\mathbf{0})$ is not directly physical[6], but it does have the appropriate quantum numbers to give a contribution to the three-particle production rate $q\bar q \to \mu^-\mu^+\gamma$, i.e. a lepton-antilepton pair together with an on-shell photon. Moreover, it is frequently measured on the lattice, which will be our most direct reference point. We will ignore the issue of overall (re)normalization in the following, and concentrate on the shape of the spectral function (meaning its ω-dependence in frequency space, or its t-dependence in coordinate space).

It is again helpful to write $S(x;\mathbf{r})$ with the NRQCD notation. The steps in eqs. (3.8), (3.9) indicate that at $\mathcal{O}(M^0)$, $S = \theta^\dagger\theta - \phi^\dagger\phi$, which does not lead to any non-trivial

[5] To 1-loop order, $M = m_{\overline{\rm MS}}(m_{\overline{\rm MS}})(1 + g^2 C_F/4\pi^2)$, $V^k_{\rm NRQCD}(x;\mathbf{0}) = V^k_{\rm QCD}(x;\mathbf{0})(1 + g^2 C_F/2\pi^2)$.

[6] It may be noted, for instance, that the scalar density requires renormalization, unlike the vector current.

t-dependence. The leading non-trivial term reads

$$S(x;\mathbf{r}) = \ldots + \frac{i}{2M}\Big[\theta^\dagger\Big(t,\mathbf{x}+\frac{\mathbf{r}}{2}\Big)\overleftrightarrow{D_j}\sigma_j\phi\Big(t,\mathbf{x}-\frac{\mathbf{r}}{2}\Big) + \\ +\phi^\dagger\Big(t,\mathbf{x}+\frac{\mathbf{r}}{2}\Big)\overleftrightarrow{D_j}\sigma_j\theta\Big(t,\mathbf{x}-\frac{\mathbf{r}}{2}\Big)\Big] + \mathcal{O}\Big(\frac{1}{M^2}\Big)\,, \qquad (3.27)$$

where $\overleftrightarrow{D_j} \equiv W\overrightarrow{D_j}(t,\mathbf{x}-\mathbf{r}/2) - \overleftarrow{D_j}(t,\mathbf{x}+\mathbf{r}/2)\,W$.

To simplify eq. (3.27) a bit, let us for now assume that the gauge fields are perturbative, so that the Wilson line can be approximated by the first term in its expansion; and that their variation is slow on the scale set by $|\mathbf{r}|$, as argued in section 3.1 (in any case, $|\mathbf{r}|$ is taken to be zero at the end). Then we may write $W \approx \mathbb{1} + ig\mathbf{r}\cdot\mathbf{A}(t,\mathbf{x})$, $\overrightarrow{D_j}(t,\mathbf{x}-\mathbf{r}/2) \approx \overrightarrow{\partial_j} - igA_j(t,\mathbf{x}) + ig\mathbf{r}\cdot\nabla A_j(t,\mathbf{x})/2$, $\overleftarrow{D_j}(t,\mathbf{x}+\mathbf{r}/2) \approx \overleftarrow{\partial_j} + igA_j(t,\mathbf{x}) + ig\mathbf{r}\cdot\nabla A_j(t,\mathbf{x})/2$. We now note that

$$\theta^\dagger\Big(t,\mathbf{x}+\frac{\mathbf{r}}{2}\Big)\overleftrightarrow{D_j}\phi\Big(t,\mathbf{x}-\frac{\mathbf{r}}{2}\Big) \simeq -2\frac{\partial}{\partial r^j}\Big\{\theta^\dagger\Big(t,\mathbf{x}+\frac{\mathbf{r}}{2}\Big)W\phi\Big(t,\mathbf{x}-\frac{\mathbf{r}}{2}\Big)\Big\}\,. \qquad (3.28)$$

Therefore, to leading order in the large-M expansion, and at least to some order in the weak-coupling expansion, we can identify

$$S(x;\mathbf{r}) \simeq -\frac{i}{M}\nabla_{\mathbf{r}}\cdot\mathbf{V}(x;\mathbf{r})\,, \qquad (3.29)$$

where the components of $\mathbf{V}$ are given in eq. (3.11).

The relation between the vector and scalar channel correlators can be pushed one step further, if we consider directly the correlators, eqs. (3.7) and (3.26). To leading order in the large-M expansion, eqs. (3.11) and (3.29) imply that

$$\begin{aligned} C^S_>(x;\mathbf{r},\mathbf{r}') &= \Big\langle S(x;\mathbf{r})S(0;-\mathbf{r}')\Big\rangle \\ &\simeq \frac{1}{M^2}\sum_{k,l=1}^{3}(\nabla_{\mathbf{r}})_k(\nabla_{\mathbf{r}'})_l\Big\langle V_k(x;\mathbf{r})V_l(0;-\mathbf{r}')\Big\rangle \\ &= \frac{1}{3M^2}\sum_{k,l=1}^{3}(\nabla_{\mathbf{r}})_k(\nabla_{\mathbf{r}'})_l\,\delta_{kl}\sum_{j=1}^{3}\Big\langle V_j(x;\mathbf{r})V_j(0;-\mathbf{r}')\Big\rangle \\ &= -\frac{1}{3M^2}\nabla_{\mathbf{r}}\cdot\nabla_{\mathbf{r}'}\sum_{j=1}^{3}\Big\langle V^j(x;\mathbf{r})V_j(0;-\mathbf{r}')\Big\rangle \\ &= -\frac{1}{3M^2}\nabla_{\mathbf{r}}\cdot\nabla_{\mathbf{r}'}\,C^V_>(x;\mathbf{r},\mathbf{r}')\,. \end{aligned} \qquad (3.30)$$

We will be making use of this important relation later on.

We now return to full QCD, and outline the computation of the 2-point scalar density correlator in eq. (3.26) at tree-level, again taking a spatial Fourier transfrom and, for generality, keeping track of a non-zero spatial momentum $\mathbf{q} \neq \mathbf{0}$ for the moment. Then,

$$C^S_E(\tau,\mathbf{q};\mathbf{r},\mathbf{r}') \\ \equiv \int \mathrm{d}^3\mathbf{x}\,e^{-i\mathbf{q}\cdot\mathbf{x}}\Big\langle\bar\psi\Big(\tau,\mathbf{x}+\frac{\mathbf{r}}{2}\Big)\psi\Big(\tau,\mathbf{x}-\frac{\mathbf{r}}{2}\Big)\;\bar\psi\Big(0,-\frac{\mathbf{r}'}{2}\Big)\psi\Big(0,+\frac{\mathbf{r}'}{2}\Big)\Big\rangle \qquad (3.31)$$

$$
\begin{aligned}
&= -N_{\mathrm{c}} \int \mathrm{d}^3\mathbf{x}\, e^{-i\mathbf{q}\cdot\mathbf{x}} \sum\!\!\!\!\!\!\int_{\tilde{P}_{\mathrm{f}},\tilde{S}_{\mathrm{f}}} e^{i(\tilde{p}_{0\mathrm{f}}-\tilde{s}_{0\mathrm{f}})\tau + i(\mathbf{s}-\mathbf{p})\cdot\mathbf{x} + i(\mathbf{s}+\mathbf{p})\cdot\frac{\mathbf{r}-\mathbf{r}'}{2}} \mathrm{Tr}\left[\frac{-i\tilde{\not{P}}+M}{\tilde{P}^2+M^2}\frac{-i\tilde{\not{S}}+M}{\tilde{S}^2+M^2}\right] \\
&= -4N_{\mathrm{c}} \sum\!\!\!\!\!\!\int_{\tilde{P}_{\mathrm{f}},\tilde{S}_{\mathrm{f}}} (2\pi)^3\delta^{(3)}(\mathbf{s}-\mathbf{p}-\mathbf{q}) e^{i(\tilde{p}_{0\mathrm{f}}-\tilde{s}_{0\mathrm{f}})\tau + i(2\mathbf{p}+\mathbf{q})\cdot\frac{\mathbf{r}-\mathbf{r}'}{2}} \frac{-\tilde{p}_{0\mathrm{f}}\tilde{s}_{0\mathrm{f}} - \mathbf{p}\cdot\mathbf{s} + M^2}{(\tilde{P}^2+M^2)(\tilde{S}^2+M^2)} \\
&= -2N_{\mathrm{c}}T^2 \sum_{\tilde{p}_{0\mathrm{f}},\tilde{s}_{0\mathrm{f}}} \int \frac{\mathrm{d}^3\mathbf{p}}{(2\pi)^3} e^{i(\tilde{p}_{0\mathrm{f}}-\tilde{s}_{0\mathrm{f}})\tau + i(2\mathbf{p}+\mathbf{q})\cdot\frac{\mathbf{r}-\mathbf{r}'}{2}} \frac{-2\tilde{p}_{0\mathrm{f}}\tilde{s}_{0\mathrm{f}} - E_{\mathbf{p}}^2 - E_{\mathbf{p}+\mathbf{q}}^2 + 4M^2 + \mathbf{q}^2}{(\tilde{p}_{0\mathrm{f}}^2 + E_{\mathbf{p}}^2)(\tilde{s}_{0\mathrm{f}}^2 + E_{\mathbf{p}+\mathbf{q}}^2)} \,.
\end{aligned}
\tag{3.32}
$$

Making use of eqs. (3.14), (3.15), this can be rewritten as

$$
\begin{aligned}
C_E^S(\tau,\mathbf{q};\mathbf{r},\mathbf{r}') = -N_{\mathrm{c}} \int \frac{\mathrm{d}^3\mathbf{p}}{(2\pi)^3} e^{i(2\mathbf{p}+\mathbf{q})\cdot\frac{\mathbf{r}-\mathbf{r}'}{2}} \times \\
\times\Bigg\{ n_{\mathrm{F}}(E_{\mathbf{p}}+\mu) n_{\mathrm{F}}(E_{\mathbf{p}+\mathbf{q}}-\mu) e^{(\beta-\tau)(E_{\mathbf{p}}+E_{\mathbf{p}+\mathbf{q}})} \left[\frac{\mathbf{q}^2+4M^2-(E_{\mathbf{p}}+E_{\mathbf{p}+\mathbf{q}})^2}{2E_{\mathbf{p}}E_{\mathbf{p}+\mathbf{q}}}\right] + \\
+ n_{\mathrm{F}}(E_{\mathbf{p}}+\mu) n_{\mathrm{F}}(E_{\mathbf{p}+\mathbf{q}}+\mu) e^{(\beta-\tau)E_{\mathbf{p}}+\tau E_{\mathbf{p}+\mathbf{q}}+\beta\mu} \left[\frac{-\mathbf{q}^2-4M^2+(E_{\mathbf{p}}-E_{\mathbf{p}+\mathbf{q}})^2}{2E_{\mathbf{p}}E_{\mathbf{p}+\mathbf{q}}}\right] + \\
+ n_{\mathrm{F}}(E_{\mathbf{p}}-\mu) n_{\mathrm{F}}(E_{\mathbf{p}+\mathbf{q}}-\mu) e^{(\beta-\tau)E_{\mathbf{p}+\mathbf{q}}+\tau E_{\mathbf{p}}-\beta\mu} \left[\frac{-\mathbf{q}^2-4M^2+(E_{\mathbf{p}}-E_{\mathbf{p}+\mathbf{q}})^2}{2E_{\mathbf{p}}E_{\mathbf{p}+\mathbf{q}}}\right] + \\
+ n_{\mathrm{F}}(E_{\mathbf{p}}-\mu) n_{\mathrm{F}}(E_{\mathbf{p}+\mathbf{q}}+\mu) e^{\tau(E_{\mathbf{p}}+E_{\mathbf{p}+\mathbf{q}})} \left[\frac{\mathbf{q}^2+4M^2-(E_{\mathbf{p}}+E_{\mathbf{p}+\mathbf{q}})^2}{2E_{\mathbf{p}}E_{\mathbf{p}+\mathbf{q}}}\right] \Bigg\} \,.
\end{aligned}
\tag{3.33}
$$

With the same considerations as between eqs. (3.16) and (3.18), the interesting part of C_E^S can be approximated as

$$
\begin{aligned}
C_E^S(\tau,\mathbf{q};\mathbf{r},\mathbf{r}') \simeq \frac{N_{\mathrm{c}}}{2M^2} \int \frac{\mathrm{d}^3\mathbf{p}}{(2\pi)^3} e^{i(2\mathbf{p}+\mathbf{q})\cdot\frac{\mathbf{r}-\mathbf{r}'}{2} - \tau\left[2M + \frac{2\mathbf{p}^2+2\mathbf{p}\cdot\mathbf{q}+\mathbf{q}^2}{2M} + \mathcal{O}\left(\frac{1}{M^3}\right)\right]} \times \\
\times \left[4\mathbf{p}^2 + 4\mathbf{p}\cdot\mathbf{q} + \mathbf{q}^2 + \mathcal{O}\left(\frac{1}{M^2}\right)\right] \,.
\end{aligned}
\tag{3.34}
$$

Note again that after these simplifications, all dependence on the temperature and on the chemical potential has disappeared from the tree-level result.

The exponential in eq. (3.34) is the same as in eq. (3.18), whereby $C_>^S$ obeys the same Schrödinger equation as $C_>^V$, eq. (3.21). The initial condition is different, however: setting $t = 0$ in eq. (3.34) (after $\tau \to it$), we find

$$
\begin{aligned}
C_>^S(0,\mathbf{q};\mathbf{r},\mathbf{r}') &= -\frac{2N_{\mathrm{c}}}{M^2}\nabla_{\mathbf{r}}^2 \int \frac{\mathrm{d}^3\mathbf{p}}{(2\pi)^3} e^{i(2\mathbf{p}+\mathbf{q})\cdot\frac{\mathbf{r}-\mathbf{r}'}{2}} + \mathcal{O}\left(\frac{1}{M^4}\right) \\
&= -\frac{2N_{\mathrm{c}}}{M^2}\nabla_{\mathbf{r}}^2\,\delta^{(3)}(\mathbf{r}-\mathbf{r}') + \mathcal{O}\left(\frac{1}{M^4}\right) \,.
\end{aligned}
\tag{3.35}
$$

This agrees, of course, with what can be deduced from eqs. (3.22), (3.30). We note that all dependence on the external momentum $\mathbf{q}$ again only appears as a part of the center-of-mass energy $2M + \mathbf{q}^2/4M$, inside eq. (3.21).

JHEP01(2008)043

For future reference, let us finally determine the spectral function, $\rho^S(\omega)$. Eq. (3.34) (after $\tau \to it$) already shows the solution of eqs. (3.21), (3.35), and we can then directly remove the point-splitting, setting $\mathbf{r}, \mathbf{r}' = \mathbf{0}$. Shifting $\mathbf{p} \to \mathbf{p} - \mathbf{q}/2$; taking the steps in footnote 4; and ignoring exponentially small terms, we find

$$\rho^S(\omega) \approx \frac{2N_{\rm c}\pi}{M^2} \int \frac{{\rm d}^3\mathbf{p}}{(2\pi)^3}\, \mathbf{p}^2\, \delta\biggl(\omega' - \frac{\mathbf{p}^2}{M}\biggr) = \frac{N_{\rm c}}{2\pi}\, \theta(\omega')\, M^{\frac{1}{2}}\, (\omega')^{\frac{3}{2}} \;, \tag{3.36}$$

where ω' is from eq. (3.24).

The analysis so far has been at tree-level. As discussed above eq. (3.28), the relation in eq. (3.30) is more general, however. Therefore, we can extract a beyond-the-leading order ρ^S by simply applying eq. (3.30) to a beyond-the-leading order ρ^V.

3.4 Other channels

In sections 3.2, 3.3, we have discussed the correlators in the vector and scalar channels. Let us now show that in the limit of a large quark mass, the correlators in the pseudoscalar and axial vector channels are to a good approximation equivalent to either of these two.

We note, first of all, that in the basis of eq. (3.10), the matrix γ_5 becomes

$$\gamma_5 = i\gamma^0\gamma^1\gamma^2\gamma^3 = \begin{pmatrix} 0 & \mathbb{1} \\ \mathbb{1} & 0 \end{pmatrix} \;. \tag{3.37}$$

Thereby the pseudoscalar density becomes

$$\begin{aligned} P(x;\mathbf{r}) &\equiv \bar{\psi}\biggl(t, \mathbf{x} + \frac{\mathbf{r}}{2}\biggr) i\gamma_5\, W\psi\biggl(t, \mathbf{x} - \frac{\mathbf{r}}{2}\biggr) \\ &= i\biggl[\theta^\dagger\biggl(t, \mathbf{x} + \frac{\mathbf{r}}{2}\biggr)\, W\phi\biggl(t, \mathbf{x} - \frac{\mathbf{r}}{2}\biggr) - \phi^\dagger\biggl(t, \mathbf{x} + \frac{\mathbf{r}}{2}\biggr)\, W\theta\biggl(t, \mathbf{x} - \frac{\mathbf{r}}{2}\biggr)\biggr] + \mathcal{O}\biggl(\frac{1}{M^2}\biggr) \,, \end{aligned} \tag{3.38}$$

where again only structures of the type $\theta^\dagger\phi$ and $\phi^\dagger\theta$ have been kept. The non-trivial two-point correlator comes from the cross-term between the two structures in eq. (3.38), and ignoring the spin-dependent corrections of $\mathcal{O}(1/M)$, a comparison with eq. (3.11) then shows that

$$C^P_>(x;\mathbf{r},\mathbf{r}') \simeq -\frac{1}{3}\, C^V_>(x;\mathbf{r},\mathbf{r}') \;, \tag{3.39}$$

where $C^P_>(x;\mathbf{r},\mathbf{r}') \equiv \langle P(x;\mathbf{r}) P(0;-\mathbf{r}')\rangle$, and $C^V_>$ is defined in eq. (3.7).

The axial vector, on the other hand, can be defined as

$$A^\mu(x;\mathbf{r}) \equiv \bar{\psi}\biggl(t, \mathbf{x} + \frac{\mathbf{r}}{2}\biggr) \gamma_5\gamma^\mu\, W\psi\biggl(t, \mathbf{x} - \frac{\mathbf{r}}{2}\biggr) \;. \tag{3.40}$$

In the case of V^μ, we found that the dominant contribution is given by the spatial components, but for the axial vector, the roles have interchanged: the leading term is

$$A^0(x;\mathbf{r}) = -\biggl[\theta^\dagger\biggl(t, \mathbf{x} + \frac{\mathbf{r}}{2}\biggr)\, W\phi\biggl(t, \mathbf{x} - \frac{\mathbf{r}}{2}\biggr) + \phi^\dagger\biggl(t, \mathbf{x} + \frac{\mathbf{r}}{2}\biggr)\, W\theta\biggl(t, \mathbf{x} - \frac{\mathbf{r}}{2}\biggr)\biggr] + \mathcal{O}\biggl(\frac{1}{M^2}\biggr) \;.$$

Comparing with eq. (3.38), we find

$$C_>^{A^0}(x;\mathbf{r},\mathbf{r}') \equiv \langle A^0(x;\mathbf{r})A^0(0;-\mathbf{r}')\rangle \simeq C_>^P(x;\mathbf{r},\mathbf{r}') \simeq -\frac{1}{3}\,C_>^V(x;\mathbf{r},\mathbf{r}')\;. \tag{3.41}$$

In lattice studies, however, attention is sometimes restricted to the spatial components A^k; repeating the previous steps, we find

$$\begin{aligned} A^k(x;\mathbf{r}) \simeq & -\frac{1}{2M}\frac{\partial}{\partial x^k}P(x,\mathbf{r}) \\ & +\frac{\epsilon_{klm}}{M}\frac{\partial}{\partial r^m}\left[\theta^\dagger\left(t,\mathbf{x}+\frac{\mathbf{r}}{2}\right)\sigma_l\,W\phi\left(t,\mathbf{x}-\frac{\mathbf{r}}{2}\right)-\phi^\dagger\left(t,\mathbf{x}+\frac{\mathbf{r}}{2}\right)\sigma_l\,W\theta\left(t,\mathbf{x}-\frac{\mathbf{r}}{2}\right)\right]\;. \end{aligned} \tag{3.42}$$

The first term is a total derivative, and the second term has a structure close to that in eq. (3.11), given that only the crossterm contributes in a correlation function. Therefore, paralleling the argument in eq. (3.30), we find

$$\begin{aligned} \int \mathrm{d}^3\mathbf{x}\, C_>^{\mathbf{A}}(x;\mathbf{r},\mathbf{r}') &\equiv \int \mathrm{d}^3\mathbf{x}\,\langle A^k(x;\mathbf{r})A^k(0;-\mathbf{r}')\rangle \\ &\simeq \frac{1}{M^2}\epsilon_{klm}\epsilon_{kl'm'}\frac{\partial^2}{\partial r^m\partial r'^{m'}}\int \mathrm{d}^3\mathbf{x}\,\langle V^l(x;\mathbf{r})V^{l'}(0;-\mathbf{r}')\rangle \\ &= -\frac{1}{3M^2}\epsilon_{klm}\epsilon_{kl'm'}\frac{\partial^2}{\partial r^m\partial r'^{m'}}\delta_{ll'}\int \mathrm{d}^3\mathbf{x}\, C_>^V(x;\mathbf{r},\mathbf{r}') \\ &= 2\int \mathrm{d}^3\mathbf{x}\, C_>^S(x;\mathbf{r},\mathbf{r}')\;. \end{aligned} \tag{3.43}$$

To summarize, eqs. (3.39), (3.41) and (3.43) show that the pseudoscalar and axial correlators do not lead to any qualitatively new structures.

4. Method to construct the spectral functions

In the previous section, we have set up the Schrödinger equation and initial conditions satisfied by the vector channel correlator $C_>^V$, and shown that the corresponding correlators in the other channels can be obtained from $C_>^V$ through various relations. The aim now is to extract the spectral functions corresponding to these correlators.

To achieve this goal, it is useful to convert the time-dependent Schrödinger equation directly to frequency space. Let

$$\psi(t;\mathbf{r},\mathbf{r}') \equiv e^{i2Mt}\,C_>^V(t,\mathbf{q};\mathbf{r},\mathbf{r}')\;, \tag{4.1}$$

and

$$\chi(t;\mathbf{r},\mathbf{r}') \equiv e^{i2Mt}C_>^S(t,\mathbf{q};\mathbf{r},\mathbf{r}') \simeq -\frac{1}{3}\,\frac{\nabla_{\mathbf{r}}\cdot\nabla_{\mathbf{r}'}}{M^2}\psi(t;\mathbf{r},\mathbf{r}')\;. \tag{4.2}$$

The corresponding frequency representations are defined by

$$\tilde\psi(\omega';\mathbf{r},\mathbf{r}') \equiv \int_{-\infty}^{\infty}\mathrm{d}t\,e^{i\omega' t}\,\psi(t;\mathbf{r},\mathbf{r}')\;,\quad \tilde\chi(\omega';\mathbf{r},\mathbf{r}') \equiv \int_{-\infty}^{\infty}\mathrm{d}t\,e^{i\omega' t}\,\chi(t;\mathbf{r},\mathbf{r}')\;, \tag{4.3}$$

and the spectral functions are then obtained from (cf. eq. (2.2))

$$\rho^V(\omega') = \lim_{\mathbf{r},\mathbf{r}'\to\mathbf{0}} \frac{1}{2}\,\tilde{\psi}(\omega';\mathbf{r},\mathbf{r}') \;, \tag{4.4}$$

$$\rho^S(\omega') = \lim_{\mathbf{r},\mathbf{r}'\to\mathbf{0}} \frac{1}{2}\,\tilde{\chi}(\omega';\mathbf{r},\mathbf{r}') \;, \tag{4.5}$$

where ω' is from eq. (3.24) and we have omitted exponentially small corrections.

We now recall from ref. [24] that the imaginary part of $V_>(t,r)$ (eq. (2.6)) is odd in $t \to -t$. Furthermore, we recall from section 3.1 that a consistent perturbative solution allows (or, to be more precise, demands) considering the limit $|t| \gg r$. Denoting

$$V_>(r) \equiv \lim_{t\to+\infty} V_>(t,r) \;, \tag{4.6}$$

the equations to be solved (eq. (2.4)) then read

$$\Big[\hat{H} - i|\,\mathrm{Im}\,V_>(r)|\Big]\psi(t;\mathbf{r},\mathbf{r}') = i\partial_t\psi(t;\mathbf{r},\mathbf{r}') \;, \quad t>0 \;, \tag{4.7}$$

$$\Big[\hat{H} + i|\,\mathrm{Im}\,V_>(r)|\Big]\psi(t;\mathbf{r},\mathbf{r}') = i\partial_t\psi(t;\mathbf{r},\mathbf{r}') \;, \quad t<0 \;, \tag{4.8}$$

where we indicated explicitly that the imaginary part is negative for $t\to+\infty$ [24, 26], and defined a Hermitean differential operator $\hat{H}$ through

$$\hat{H} \equiv -\frac{\nabla^2_{\mathbf{r}}}{M} + \mathrm{Re}\,V_>(r) \;. \tag{4.9}$$

Since the effective Hamiltonian is time-independent both for $t<0$ and for $t>0$, we can formally solve eqs. (4.7), (4.8):

$$\psi(t;\mathbf{r},\mathbf{r}') = \begin{cases} e^{-i\hat{H}t-|\mathrm{Im}\,V_>(r)|t}\,\psi(0;\mathbf{r},\mathbf{r}') & , \quad t>0 \\ e^{-i\hat{H}t+|\mathrm{Im}\,V_>(r)|t}\,\psi(0;\mathbf{r},\mathbf{r}') & , \quad t<0 \end{cases} \;, \tag{4.10}$$

where, according to eqs. (3.22), (4.1),

$$\psi(0;\mathbf{r},\mathbf{r}') = -6N_{\mathrm{c}}\delta^{(3)}(\mathbf{r}-\mathbf{r}') \;. \tag{4.11}$$

Taking a Fourier-transform, we get

$$\begin{aligned}
\tilde{\psi}(\omega';\mathbf{r},\mathbf{r}') &= \int_{-\infty}^{\infty}\mathrm{d}t\,e^{i\omega' t}\psi(t;\mathbf{r},\mathbf{r}') \\
&= \Bigg\{\Big[i\omega' - i\hat{H} - |\,\mathrm{Im}\,V_>(r)|\Big]^{-1}\,e^{it(\omega'-\hat{H})-|\mathrm{Im}\,V_>(r)|t}\Big|_0^{\infty} + \\
&\qquad + \Big[i\omega' - i\hat{H} + |\,\mathrm{Im}\,V_>(r)|\Big]^{-1}\,e^{it(\omega'-\hat{H})+|\mathrm{Im}\,V_>(r)|t}\Big|_{-\infty}^{0}\Bigg\}\,\psi(0;\mathbf{r},\mathbf{r}') \\
&= \frac{1}{i}\Big\{\Big[\omega' - \hat{H} - i|\,\mathrm{Im}\,V_>(r)|\Big]^{-1} - \Big[\omega' - \hat{H} + i|\,\mathrm{Im}\,V_>(r)|\Big]^{-1}\Big\}\,\psi(0;\mathbf{r},\mathbf{r}') \;.
\end{aligned} \tag{4.12}$$

To give a concrete meaning to the inverses in eq. (4.12), we define a function $\tilde{\Psi}(\omega';\mathbf{r},\mathbf{r}')$ as the solution of the equation

$$\left[\omega' - \hat{H} + i|\operatorname{Im} V_>(r)|\right]\tilde{\Psi}(\omega';\mathbf{r},\mathbf{r}') = -6N_{\mathrm{c}}\delta^{(3)}(\mathbf{r}-\mathbf{r}') \; . \tag{4.13}$$

Then the result of eq. (4.12) can be rewritten as

$$\tilde{\psi}(\omega';\mathbf{r},\mathbf{r}') = -2\operatorname{Im}\left[\tilde{\Psi}(\omega';\mathbf{r},\mathbf{r}')\right] \; . \tag{4.14}$$

According to eqs. (4.2), (4.4), (4.5), the spectral functions are now obtained from

$$\rho^V(\omega') = -\lim_{\mathbf{r},\mathbf{r}'\to\mathbf{0}} \operatorname{Im}\left[\tilde{\Psi}(\omega';\mathbf{r},\mathbf{r}')\right] \; , \tag{4.15}$$

$$\rho^S(\omega') \simeq \lim_{\mathbf{r},\mathbf{r}'\to\mathbf{0}} \frac{1}{3M^2}\operatorname{Im}\left[\nabla_{\mathbf{r}}\cdot\nabla_{\mathbf{r}'}\tilde{\Psi}(\omega';\mathbf{r},\mathbf{r}')\right] \; . \tag{4.16}$$

To summarize, we have reduced the determination of the spectral functions to the solution of a time-independent inhomogeneous Schrödinger equation, eq. (4.13).

As the next step, following ref. [36], we introduce the ansatz

$$\tilde{\Psi}(\omega';\mathbf{r},\mathbf{r}') \equiv \sum_{l=0}^{\infty}\sum_{m=-l}^{l}\frac{\tilde{g}_l(\omega';r,r')}{rr'}Y_{lm}(\Omega)Y^*_{lm}(\Omega') \; . \tag{4.17}$$

Here Y_{lm} are the spherical harmonics, normalised as $\int \mathrm{d}\Omega\, Y^*_{lm}(\Omega)Y_{l'm'}(\Omega) = \delta_{ll'}\delta_{mm'}$, where $\mathrm{d}\Omega = \mathrm{d}\cos\theta\,\mathrm{d}\phi$, and satisfying

$$\sum_{lm} Y^*_{lm}(\Omega')Y_{lm}(\Omega) = \delta(\Omega-\Omega') \equiv \delta(\cos\theta-\cos\theta')\,\delta(\phi-\phi') \; . \tag{4.18}$$

The δ-function can be written as

$$\delta^{(3)}(\mathbf{r}-\mathbf{r}') = \frac{1}{rr'}\delta(r-r')\delta(\Omega-\Omega') \; , \tag{4.19}$$

whereby eq. (4.13) becomes

$$\left[\omega' - \hat{H}_r + i|\operatorname{Im} V_>(r)|\right]\tilde{g}_l(\omega';r,r') = -6N_{\mathrm{c}}\delta(r-r') \; , \tag{4.20}$$

with

$$\hat{H}_r \equiv -\frac{1}{M}\frac{\partial^2}{\partial r^2} + \frac{l(l+1)}{Mr^2} + \operatorname{Re} V_>(r) \; . \tag{4.21}$$

The remaining goal is to reduce the problem to the solution of the homogeneous equation. Following refs. [36, 8], we introduce the ansatz

$$\tilde{g}_l \equiv A\, g^l_<(r_<)g^l_>(r_>) \; , \tag{4.22}$$

where $g^l_<$ is a solution of the homogeneous equation regular at zero; $g^l_>$ is a solution of the homogeneous equation regular at infinity; and $r_< = \min(r,r'), r_> = \max(r,r')$.

Obviously, the function $\tilde{g}_l$ is symmetric in $r \leftrightarrow r'$, and continuous at $r = r'$. Given the well-known form of the solution $g^l_<$, it must thus behave as

$$\tilde{g}_l \sim [r^{l+1} + \mathcal{O}(r^{l+2})][(r')^{l+1} + \mathcal{O}((r')^{l+2})] \tag{4.23}$$

at small r, r'. For the vector channel spectral function, eqs. (4.15), (4.17) now imply that

$$\rho^V(\omega') = -\lim_{r,r'\to 0} \frac{1}{4\pi r r'} \operatorname{Im}\Big[\tilde{g}_0(\omega'; r, r')\Big] \,, \tag{4.24}$$

i.e. that only the S-wave ($l = 0$) solution of the homogeneous part of eq. (4.20) contributes.

Consider then the scalar channel. According to eq. (4.16), the scalar channel spectral function can be extracted from the same function $\tilde{\Psi}$ as the vector channel one, by taking two derivatives and then extrapolating $r, r' \to 0$. Inspecting eq. (4.23), we see that we at least get a contribution from the P-wave ($l = 1$). However, according to eq. (4.23), it is also possible to get a contribution from the *subleading S-wave terms*, $\tilde{g}_0 \sim [r + \mathcal{O}(r^2)][r' + \mathcal{O}((r')^2)]$. As far as we can see, this contribution was omitted in ref. [8].

We relegate a more detailed discussion on how to write the solutions for the spectral functions ρ^V, ρ^S to appendix A, given that the further steps are quite technical in nature, and give here just the final formulae. Introducing the dimensionless variables $\varrho \equiv r\alpha M$ and $\alpha \equiv g^2 C_F/4\pi$, the vector channel spectral function from eq. (4.24) can be simplified to

$$\frac{\rho^V(\omega')}{M^2} = -\frac{6N_{\rm c}\alpha}{4\pi} \lim_{\delta\to 0} \int_\delta^\infty \mathrm{d}\varrho \operatorname{Im}\left\{\frac{1}{[g^0_<(\varrho)]^2}\right\}\Bigg|_{g^0_<(\varrho)=\varrho-\varrho^2/2+\ldots} \,, \tag{4.25}$$

while the scalar channel spectral function becomes

$$\frac{\rho^S(\omega')}{M^2} = \frac{N_{\rm c}\alpha^3}{8\pi} \lim_{\delta\to 0} \int_\delta^\infty \mathrm{d}\varrho \operatorname{Im}\left\{\frac{1}{[g^0_<(\varrho)]^2} + \frac{36}{[g^1_<(\varrho)]^2}\right\}\Bigg|_{g^1_<(\varrho)=\varrho^2-\varrho^3/4+\ldots} \,. \tag{4.26}$$

We remark that because of the factor 36, the first (S-wave) term is numerically subdominant in eq. (4.26), and would be totally negligible, were it not for the fact that is does lead to a resonance peak, unlike the second term.

5. Numerical results

In the previous section, we have reduced the numerical determination of the vector and scalar channel spectral functions to eqs. (4.25), (4.26), respectively. In these equations the functions $g^l_<$, $l = 0, 1$, denote the regular solutions of the homogeneous part of eq. (4.20),

$$\Big[\omega' - \hat{H}_r + i|\operatorname{Im} V_>(r)|\Big] g^l_< = 0 \,, \tag{5.1}$$

where $\hat{H}_r$ is from eq. (4.21). Further details can be found in appendix A.

In practice, the procedure of determining ρ^V, ρ^S starts from some small value, $\varrho \equiv \delta$, with for instance $\delta = 10^{-2}$, at which point we impose as initial conditions the properties of the regular solutions at small ϱ, $g^0_<(\delta) = \delta - \delta^2/2 + \ldots$, $g^1_<(\delta) = \delta^2 - \delta^3/4 + \ldots$.

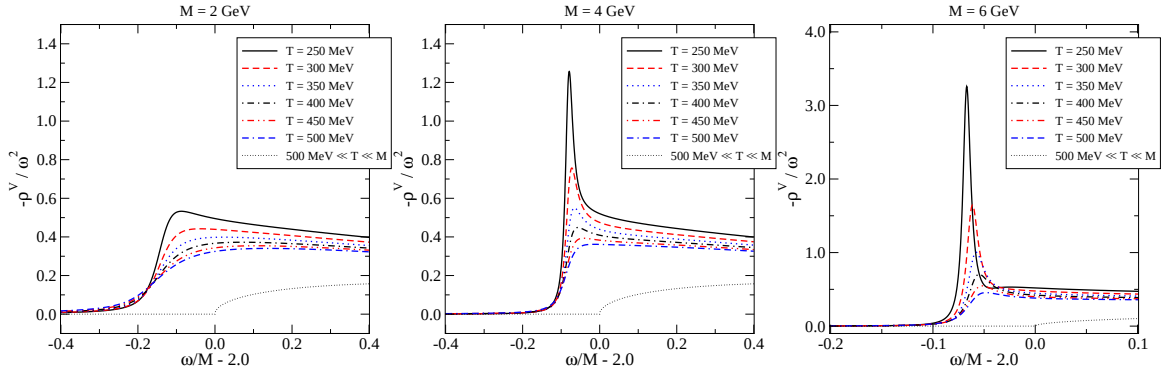

Figure 1: The resummed perturbative vector channel spectral function $\rho^V(\omega)$, in units of ω^2, in the non-relativistic regime, $(\omega - 2M)/M \ll 1$, for $M = 2, 4, 6\,\mathrm{GeV}$ (from left to right). To the order considered, M is the heavy quark pole mass. Note that for better visibility, the axis ranges are different in the rightmost figure.

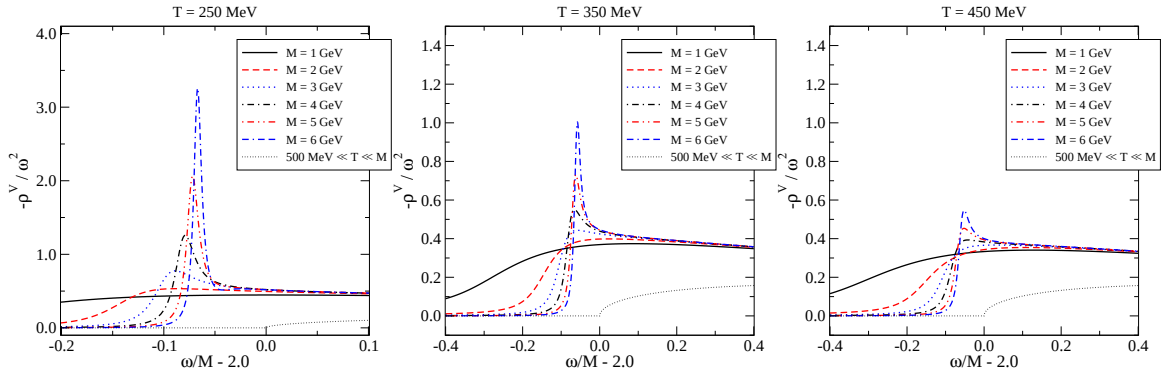

Figure 2: The resummed perturbative vector channel spectral function $\rho^V(\omega)$, in units of ω^2, in the non-relativistic regime, $(\omega - 2M)/M \ll 1$, for $T = 250, 350, 450\,\mathrm{MeV}$ (from left to right). To the order considered, M is the heavy quark pole mass. Note that for better visibility, the axis ranges are different in the leftmost figure.

We then integrate eq. (5.1) towards larger ϱ, constructing simultaneously the quantities in eqs. (4.25), (4.26). After a while, $g^0_<(\varrho)$ and $g^1_<(\varrho)$ start to grow rapidly and the integrals in eqs. (4.25), (4.26) settle to their asymptotic values. Subsequently, we check that the results obtained are independent of the starting point δ. The numerics is straightforward and poses no problems.

Apart from the pole mass M, the solution depends on what is plugged in for g^2 and m_{D}. We employ here simple analytic expressions that can be extracted from ref. [37],

$$g^2 \simeq \frac{8\pi^2}{9\ln(9.082\,T/\Lambda_{\overline{\mathrm{MS}}})}\,, \quad m_{\mathrm{D}}^2 \simeq \frac{4\pi^2 T^2}{3\ln(7.547\,T/\Lambda_{\overline{\mathrm{MS}}})}\,, \qquad \text{for } N_{\mathrm{c}} = N_{\mathrm{f}} = 3, \mu = 0\,. \quad (5.2)$$

We also fix $\Lambda_{\overline{\mathrm{MS}}} \simeq 300\,\mathrm{MeV}$; for the uncertainties related to this, see figure 2 of ref. [24].

JHEP01(2008)043

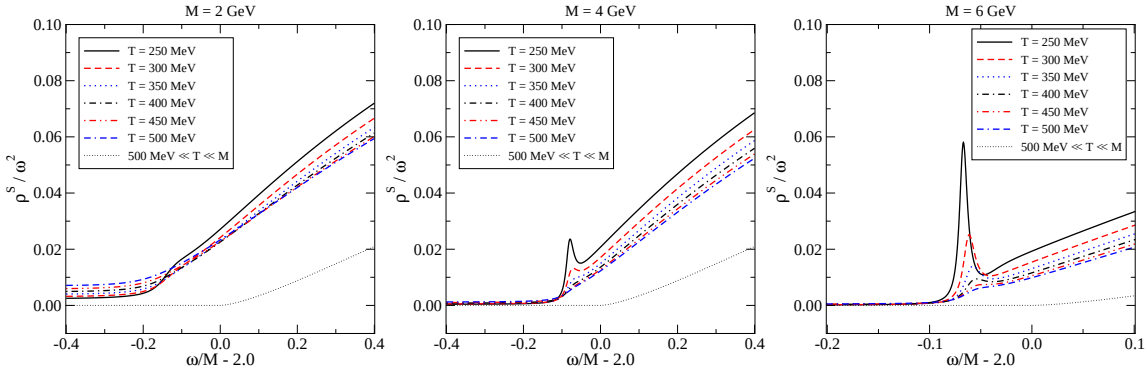

Figure 3: The resummed perturbative scalar channel spectral function $\rho^S(\omega)$, in units of ω^2, in the non-relativistic regime, $(\omega - 2M)/M \ll 1$, for $M = 2, 4, 6\,\mathrm{GeV}$ (from left to right). To the order considered, M is the heavy quark pole mass. Note that for better visibility, the range of x-axis is different in the rightmost figure.

The results for $-\rho^V/\omega^2$ (eq. (4.25) divided by $-\omega^2/M^2$) are shown in figures 1, 2, and those for ρ^S/ω^2 (eq. (4.26) divided by ω^2/M^2) in figures 3, 4. The results are given in a range of ω where relativistic corrections, i.e. terms of higher order in a Taylor expansion in $(\omega - 2M)/M$, are estimated to be at most at the 10% level. We show a scan of mass values, given that the inherent theoretical uncertainties of the charm and bottom pole masses are several hundred MeV (for a pedagogic discussion, see ref. [39]), and that in lattice simulations there are further uncertainties, related to scale setting etc, which make it difficult to sit precisely at the physical point. As far as the other channels are concerned, we recall from eqs. (3.39), (3.41), (3.43) that

$$\rho^P \simeq -\frac{1}{3}\,\rho^V \;; \quad \rho^{A^0} \simeq -\frac{1}{3}\,\rho^V \;; \quad \rho^{\mathbf{A}} \simeq 2\rho^S \;. \tag{5.3}$$

5.1 Comparison with lattice

As of today, lattice reconstructions of the spectral functions in various channels [4–6] suffer from significant uncertainties. Apart from the usual problems, it may be mentioned that the Compton wavelength associated with the heavy quarks tends to be of the order of the lattice spacing, so that we may expect even more significant discretization artifacts than in the usual quenched or 2+1 light flavour simulations; and that the analytic continuation from Euclidean lattice data to the Minkowskian spectral function necessarily involves model input, whose uncertainties are difficult to quantify. Nevertheless, it has been claimed that the latter types of uncertainties may be under reasonable control from a practical point of view [40]. The most recent lattice results in this spirit can be found in refs. [5, 6].

It has become fashionable recently not to compare directly the spectral functions, but the Euclidean correlators for which direct lattice data exists. Though this removes the uncertainties related to the analytic continuation, it also comes with a heavy price: most of the structure in a Euclidean correlator is determined by values of ω far from the threshold,

JHEP01(2008)043

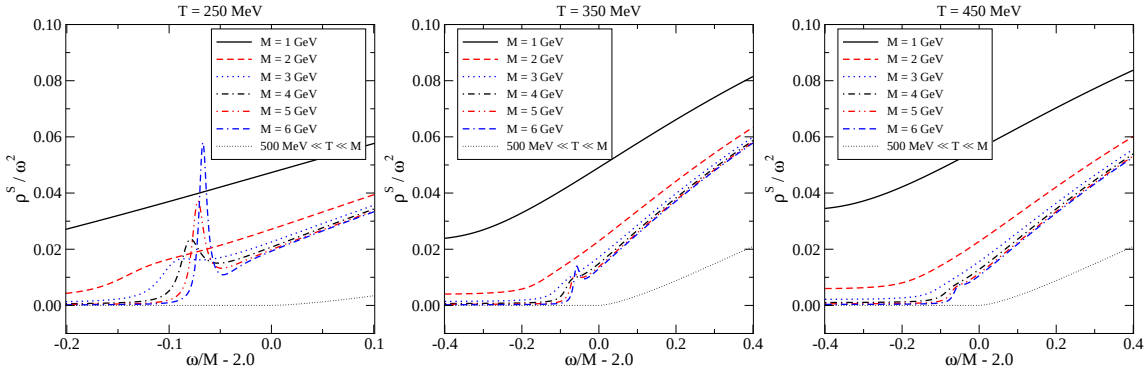

Figure 4: The resummed perturbative scalar channel spectral function $\rho^S(\omega)$, in units of ω^2, in the non-relativistic regime, $(\omega - 2M)/M \ll 1$, for $T = 250, 350, 450\,\mathrm{MeV}$ (from left to right). To the order considered, M is the heavy quark pole mass. Note that for better visibility, the range of x-axis is different in the leftmost figure.

$\omega \ll 2M$ or $\omega \gg 2M$, so that the actual physics we are interested in tends to be hidden in tiny effects somewhere in the middle of the Euclidean time interval. For this reason, we do not consider Euclidean correlators to be as interesting as the spectral functions, and touch only the latter in the following.

Most of the lattice data exists for the charmonium case. The temperatures where the charmonium peak disappears from the spectral function are rather low, however; in fact they are in a regime where our analysis is probably not yet justified. Assuming the charmonium pole mass to be in the range $M \sim (1.5 \ldots 2.0)\,\mathrm{GeV}$, we nevertheless observe from figure 1(left) that at $T \approx 250\,\mathrm{MeV}$ a certain "enhancement" can still be seen in the vector (and thus, in the pseudoscalar) channel. This then disappears at higher temperatures. In contrast, in the scalar channel, figure 3(left), there is practically no structure. These observations are certainly not in conflict with the lattice results of refs. [5, 6]. Furthermore, we may note that the absolute magnitudes of ρ_V and ρ_S in figures 1(left), 3(left) are qualitatively in a similar relation to each other as the spectral functions measured on the lattice: the difference of about an order of magnitude is due to the $1/M^2$-suppression in the scalar case. At the same time, it needs to be kept in mind that in the scalar case the operators require renormalization, and that we have in any case not computed radiative corrections to the absolute magnitudes of the spectral functions, so that the comparison cannot be taken too seriously.

Data for the bottomonium case, where our predictions should be more reliable, can be found in ref. [5]. There is again an inherent uncertainty of several hundred MeV in the bottom quark pole mass, but realistic values are presumable in the range $M \sim (4.5 \ldots 5.0)\,\mathrm{GeV}$. According to figures 1, 2 (middle to right), there is now a clear peak in the vector channel spectral function, up to a temperature of perhaps 500 MeV. In the scalar channel case, figures 3, 4 (middle to right), the structure is much less pronounced, but a tiny enhancement can be observed up to a temperature of about 400 MeV. These results are qualitatively in better agreement with the lattice data in ref. [5] than the potential model results of ref. [8],

JHEP01(2008)043

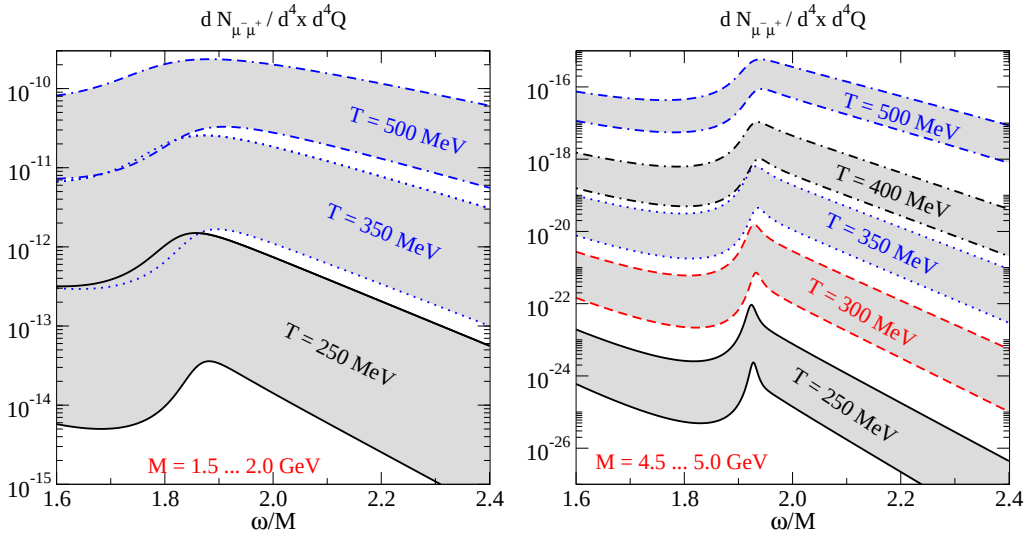

Figure 5: The physical dilepton production rate, eq. (2.3), from charmonium (left) and bottomonium (right), as a function of the energy, for various temperatures. The mass M corresponds to the pole mass, and is subject to uncertainties of several hundred MeV; we use the intervals 1.5...2.0 GeV and 4.5...5.0 GeV to illustrate the magnitude of the corresponding error bands. The low mass corresponds to the upper edge of each error band.

where no peak was found in the scalar channel case; as we have explained in section 4, the discrepancy can be traced back to a difference in the reconstruction of the spectral function from a Schrödinger equation. Nevertheless, in practice, it should again be stressed that systematic uncertainties of the lattice data are certainly too large to make a quantitative comparison.

5.2 Dilepton rate

Apart from the spectral functions, it is interesting to plot also the physical observable, the dilepton production rate given in eq. (2.3). This is shown in figure 5. The significant difference with respect to the vector channel spectral function is the existence of the Boltzmann factor (or, to be more precise, Bose-Einstein factor) in eq. (2.3). Obviously, for a fixed frequency around the threshold, $\omega \sim 2M$, the Boltzmann factor $\exp(-\omega/T) \sim \exp(-2M/T)$ introduces a strong dependence of the dilepton rate on the temperature or, for a given temperature, on the mass. The exponential boosts the rate at high temperatures, and makes it decrease rapidly at large frequencies. Thereby the dilepton rate shows a much stronger resonance-like behaviour than the spectral function, figure 1. In particular, some kind of a peak structure remains visible in the dilepton rate in figure 5 even at temperatures which are so high that there is only a smooth step-like behaviour visible in the spectral function in figure 1.

JHEP01(2008)043

6. Physical picture of heavy quarkonium in a thermal plasma

Conceptually, the most important difference between our analysis and traditional potential models [7, 8] is the existence of an imaginary part in the static potential, eq. (2.6). Physically, the imaginary part implies that quarkonium at high temperatures should not be thought of as a stationary state. Rather, the norm of its wave function decays exponentially with (Minkowski) time. This is due to the fact that, apart from experiencing Debye screening, there is also a finite probability for the off-shell gluons binding the two quarks to disappear, due to Landau damping, i.e. inelastic scatterings with hard particles in the plasma. Once $T \sim gM$, the imaginary part is in fact parametrically larger than the binding energy (cf. section 3.1). At the same time, for low enough temperatures, $T \sim g^2 M$, the imaginary part plays a subdominant role (cf. section 3.1).

It may be useful to remark that if, on the contrary, one goes to a Euclidean lattice, then a non-zero wave function *can* be defined at any finite value of the "imaginary time" coordinate τ, $0 < \tau < \beta$. Introducing also gauge-fixing, such wave functions have been measured with Monte Carlo simulations in ref. [34] (for a recent review, see ref. [35]). With regard to the discussion above, the physical significance of such wave functions for Minkowski-time observables is not obvious; hence we do not discuss them here.

7. Conclusions

The purpose of this paper has been to experiment, as generally as possible, with the resummed perturbative framework that was introduced in refs. [24, 25], in order to offer one more handle on the properties of heavy quarkonium in hot QCD, thus supplementing the traditional approaches based on potential models and on lattice QCD.

The key ingredient of our approach is a careful definition of a finite-temperature real-time static potential that can be inserted into a Schrödinger equation obeyed by certain heavy quarkonium Green's functions. The potential in question, denoted by $\lim_{t\to\infty} V_>(t,r)$, has both a real and an imaginary part (cf. eq. (2.6)). An important conceptual consequence from the existence of an imaginary part is that heavy quarkonium should not be thought of as a stationary state at high temperatures, but as a short-lived transient, with the quark and antiquark binding together only for a brief moment before unattaching again.

On the more technical level we have noted that, in terms of eq. (4.17), the vector channel spectral function gets a contribution only from the S-wave, $l = 0$, while the scalar channel spectral function gets a contribution both from the S-wave and P-wave, $l = 0, 1$. Here we differ from the potential model analysis in ref. [8] where, as far as we can see, only $l = 1$ was considered for the scalar channel. The reason for the difference is discussed at the end of section 4. The difference is significant, since the S-wave contribution introduces a small reasonance peak to the scalar channel spectral function as well.

The phenomenological pattern we find for the spectral functions within this framework is not too different from indications from lattice QCD: scalar channel charmonium displays practically no reasonance peak above a temperature of 200 MeV; vector channel

JHEP01(2008)043

charmonium has some peak-like structure up to a temperature of about 300 MeV; scalar channel bottomonium is again weakly bound but does show a small enhancement up to a temperature of about 400 MeV; vector channel bottomonium can support a resonance peak up to a temperature of about 500 MeV. (Because of unknown higher order corrections, these numbers are subject to uncertainties of several tens of MeV.)

At the same time, we stress that in the physical dilepton rate, figure 5, the quarkonium peak always becomes *more pronounced* with increasing temperature, irrespective of the disappearance of the resonance structure from the spectral function. This boost is due to an interplay of the free quark continuum in the spectral function, and the Boltzmann factor $\exp(-\omega/T)$.

There are a few directions in which our work could be extended, in order to go beyond a purely perturbative approach. In particular, the imaginary part of the real-time static potential has been measured with classical lattice gauge theory simulations in ref. [26], and could thus to some extent be used in a non-perturbative setting. Hopefully, the real part of our static potential could also be related to quantities that are measurable with lattice Monte Carlo methods, thereby allowing us to probe more reliably the phenomenologically interesting temperature regime around a few hundred MeV.

Acknowledgments

M.L. thanks T. Hatsuda and S. Kim for useful suggestions, and the Isaac Newton Institute for Mathematical Sciences, where part of this work was carried out, for hospitality. This work was partially supported by the BMBF project *Hot Nuclear Matter from Heavy Ion Collisions and its Understanding from QCD*.

A. Numerical method for finding the spectral functions

In this appendix we provide details concerning the numerical method that we have used for determining the vector and scalar channel spectral functions. The basic approach is from ref. [36], where it was applied for the vector channel at zero temperature; the method was extended to the scalar channel case in ref. [8]. Our presentation is rather close to that in ref. [8], but we choose to spell out the details anew due to the fact that, as already mentioned in section 4, we find one additional term in the scalar channel case. Furthermore, the existence of an imaginary part in our static potential simplifies certain points of the analysis. We should point out that the method presented here appears to be numerically superior to that introduced for the vector channel in ref. [25].

A.1 Vector channel

We proceed with the evaluation of eq. (4.24). Given the ansatz in eq. (4.22), it remains to determine $A, g^l_<, g^l_>$, and then to extrapolate $r, r' \to 0$. We thus need to know, in particular, the asymptotic behaviours of the functions $g^l_<, g^l_>$ near the origin. Let $g^l_{\rm r}$ and $g^l_{\rm i}$ be the

solutions regular and irregular around the origin, respectively:

$$g_{\rm r}^l = r^{l+1}\sum_{n=0}^{\infty} a_n r^n \approx a_0 r^{l+1} \;, \tag{A.1}$$

$$g_{\rm i}^l = g_{\rm r}^l(r)\int_\delta^r {\rm d}r'\,\frac{1}{[g_{\rm r}^l(r')]^2} \approx -\frac{1}{a_0}\frac{r^{-l}}{2l+1} \;. \tag{A.2}$$

We may then choose

$$g_<^l(r) = g_{\rm r}^l(r) \;, \tag{A.3}$$

$$g_>^l(r) = g_{\rm i}^l(r) + B^l g_{\rm r}^l(r) \;, \tag{A.4}$$

where the coefficient B^l is defined such as to guarantee the regularity of $g_>^l(r)$ at infinity,

$$B^l = -\lim_{r\to\infty}\frac{g_{\rm i}^l(r)}{g_{\rm r}^l(r)} = -\int_\delta^\infty {\rm d}r'\,\frac{1}{[g_{\rm r}^l(r')]^2} \;. \tag{A.5}$$

Combining eqs. (A.2), (A.4), (A.5), we can write

$$g_>^l(r) = -g_{\rm r}^l(r)\int_r^\infty {\rm d}r'\,\frac{1}{[g_{\rm r}^l(r')]^2} \;. \tag{A.6}$$

Let us next compute the coefficient A in eq. (4.22). Integrating both sides of eq. (4.20) with $\int_{r'-0^+}^{r'+0^+}{\rm d}r\,(\ldots)$, yields

$$A = \frac{6N_{\rm c}M}{g_>^l(r'){\rm d}g_<^l(r')/{\rm d}r' - g_<^l(r'){\rm d}g_>^l(r')/{\rm d}r'} \;. \tag{A.7}$$

Involving a Wronskian, this expression is independent of the position r' at which it is evaluated, so we can do this at small r'. Then we can use the asymptotic forms from eqs. (A.1), (A.2), to find that

$$A = -6N_{\rm c}M \;. \tag{A.8}$$

Note that this expression is independent of l.

We finally take the limit $r, r' \to 0$, while keeping $r < r'$, so that $r_< \equiv r$, $r_> \equiv r'$. Inserting eqs. (4.22), (A.1), and (A.8) into eq. (4.24), yields

$$\begin{aligned}\rho^V(\omega') &= \frac{6N_{\rm c}M}{4\pi}\lim_{r,r'\to 0}\frac{1}{rr'}\,{\rm Im}\Big[g_>^0(r')g_<^0(r)\Big] \\ &= -\frac{6N_{\rm c}Ma_0}{4\pi}\lim_{r'\to 0}{\rm Im}\bigg\{\frac{g_{\rm r}^0(r')}{r'}\int_{r'}^\infty {\rm d}r''\,\frac{1}{[g_{\rm r}^0(r'')]^2}\bigg\} \;,\end{aligned} \tag{A.9}$$

where we assumed a_0 to be real.

Let us now analyse the origin of the imaginary part in eq. (A.9). It will be convenient to express the r-dependence in terms of the dimensionless variable $\varrho \equiv r\alpha M$, where $\alpha \equiv g^2 C_F/4\pi$. In these units, the homogeneous Schrödinger equation (eq. (5.1)) reads

$$\bigg[\frac{\partial^2}{\partial\varrho^2} - \frac{l(l+1)}{\varrho^2} + \frac{1}{\varrho} + \mathcal{O}(1)\bigg] g_{\rm r}^l(\varrho) = 0 \;, \tag{A.10}$$

implying

$$g_{\rm r}^l(\varrho) = \varrho^{l+1} - \frac{1}{2(l+1)}\varrho^{l+2} + \dots \; . \tag{A.11}$$

At some order the solution also develops an imaginary part; let us write an ansatz

$$g_{\rm r}^l(\varrho) = \varrho^{l+1} - \frac{1}{2(l+1)}\varrho^{l+2} + \ldots + i\gamma_1\varrho^x \; , \quad \gamma_1 \in \mathbb{R} \; . \tag{A.12}$$

The imaginary part in eq. (4.20) behaves as $\sim i\gamma_2\varrho^2$ at small ϱ. Inserting into the Schrödinger equation, we get for the leading imaginary term

$$i\gamma_1\varrho^{x-2}[x(x-1) - l(l+1)] + i\gamma_2\varrho^2 \cdot \varrho^{l+1} = 0 \; , \tag{A.13}$$

implying $x = l+5$.

Returning to eq. (A.9), there are in principle two possibilities for the origin of the imaginary part. However, according to eqs. (A.11), (A.13), $\lim_{r'\to 0}\mathrm{Im}[g_{\rm r}^0/r'] \int_{r'}^\infty \mathrm{d}r'' \,\mathrm{Re}\{1/[g_{\rm r}^0(r'')]^2\} \sim \lim_{r'\to 0}(r')^4/(r') = 0$. Therefore the imaginary part can only arise from $\mathrm{Im}\{1/[g_{\rm r}^0(r'')]^2\}$. Inserting the asymptotic form of $\mathrm{Re}[g_{\rm r}^0/r']$ from eq. (A.11); using the variable ϱ; and noting that this corresponds to the choice $a_0 = \alpha M$, we then obtain eq. (4.25).

It is useful to crosscheck that eq. (4.25) produces the correct result in the free limit. In the free case there is no $i|\,\mathrm{Im}\,V_>(r)|$ in eq. (4.20), and a factor $i\epsilon \equiv i0^+$ needs to be inserted instead, to pick up the correct (retarded) solution. In dimensionless units, the homogeneous equation then becomes

$$\left[\frac{\partial^2}{\partial\varrho^2} + \frac{\hat\omega'}{\alpha^2} + i\epsilon\right] g_{\rm r}^0(\varrho) = 0 \; , \tag{A.14}$$

where $\hat\omega' \equiv \omega'/M$. We denote

$$k \equiv \sqrt{\frac{\hat\omega'}{\alpha^2} + i\epsilon} \; . \tag{A.15}$$

The solution with the correct behaviour around the origin (with $a_0 = \alpha M$) reads

$$g_{\rm r}^0(\varrho) = \frac{1}{k}\sin(k\varrho) \; . \tag{A.16}$$

We can write

$$\frac{1}{[g_{\rm r}^0(\varrho')]^2} = -k\frac{\mathrm{d}}{\mathrm{d}\varrho'}\left\{\frac{\cos(k\varrho')}{\sin(k\varrho')}\right\} \; . \tag{A.17}$$

The integral in eq. (4.25) can now be carried out; the substitution at the upper end gives a contribution from the exponentially growing terms $\exp(-ik\varrho')$, present both in the cosine and in the sine. Their ratio gives $-i$, and the total is then

$$\frac{\rho^V(\omega')}{M^2} = -\frac{6N_{\rm c}\alpha}{4\pi}\,\mathrm{Im}\left\{\left(\frac{\hat\omega'}{\alpha^2} + i\epsilon\right)^{\frac{1}{2}} i\right\} = -\frac{3N_{\rm c}}{2\pi}\,\theta(\omega')\,(\hat\omega')^{1/2} \; . \tag{A.18}$$

This indeed agrees with eq. (3.23).

A.2 Scalar channel

In the scalar channel case, the equations to be solved are (4.16), (4.17), (4.20); the ansatz for the solution is in eq. (4.22), with A given by eq. (A.8).

Let us first work out the contribution from the mode $l = 0$ (S-wave). According to eqs. (4.17), (4.22), (A.3), (A.6), the relevant term of $\tilde{\Psi}$, denoted by $\delta_o\tilde{\Psi}$, is

$$\delta_0\tilde{\Psi}(\omega';\mathbf{r},\mathbf{r}') = -\frac{1}{4\pi rr'}A\,g^0_{\rm r}(r)g^0_{\rm r}(r')\int_{r'}^{\infty}{\rm d}r''\,\frac{1}{[g^0_{\rm r}(r'')]^2}\;. \tag{A.19}$$

Inserting into eq. (4.16), making use of eq. (A.8), and going over into the dimensionless variable ϱ, we get

$$\frac{\delta_0\rho^S(\omega')}{M^2} = \frac{2N_{\rm c}\alpha^3}{4\pi}\lim_{\varrho,\varrho'\to 0}{\rm Im}\biggl\{\frac{\rm d}{{\rm d}\varrho}\biggl(\frac{g^0_{\rm r}(\varrho)}{\varrho}\biggr)\frac{\rm d}{{\rm d}\varrho'}\biggl(\frac{g^0_{\rm r}(\varrho')}{\varrho'}\int_{\varrho'}^{\infty}{\rm d}\varrho''\,\frac{1}{[g^0_{\rm r}(\varrho'')]^2}\biggr)\biggr\}\;. \tag{A.20}$$

According to eq. (A.11), the first term inside the curly brackets is $\lim_{\varrho\to 0}{\rm d}_\varrho(g^0_{\rm r}/\varrho) = -1/2$, so that we get

$$\frac{\delta_0\rho^S(\omega')}{M^2} = -\frac{N_{\rm c}\alpha^3}{4\pi}\lim_{\varrho'\to 0}{\rm Im}\biggl\{\frac{\rm d}{{\rm d}\varrho'}\biggl(\frac{g^0_{\rm r}(\varrho')}{\varrho'}\int_{\varrho'}^{\infty}{\rm d}\varrho''\,\frac{1}{[g^0_{\rm r}(\varrho'')]^2}\biggr)\biggr\}\;. \tag{A.21}$$

In principle there are again two possible origins for the imaginary part. However, as we saw in the vector channel case, ${\rm Im}[g^0_{\rm r}/\varrho']\int_{\varrho'}^{\infty}{\rm d}\varrho''\,{\rm Re}\{1/[g^0_{\rm r}(\varrho'')]^2\} \sim (\varrho')^3$, so that a non-zero contribution can only arise from ${\rm Im}\{1/[g^0_{\rm r}(\varrho'')]^2\}$. Furthermore, the derivative can only act on the combination multiplying the integral, since

$$\frac{{\rm Re}[g^0_{\rm r}(\varrho')]}{\varrho'}\,{\rm Im}\biggl\{\frac{1}{[g^0_{\rm r}(\varrho')]^2}\biggr\} \approx {\rm Im}\biggl\{\frac{1}{[g^0_{\rm r}(\varrho')]^2}\biggr\} \approx {\rm Im}\biggl\{\frac{1}{(\varrho')^2+2i\gamma_1(\varrho')^6}\biggr\} \approx -2\gamma_1(\varrho')^2\;. \tag{A.22}$$

Making use of $\lim_{\varrho'\to 0}{\rm d}_{\varrho'}(g^0_{\rm r}/\varrho') = -1/2$, the S-wave contribution to the scalar spectral function thus becomes

$$\frac{\delta_0\rho^S(\omega')}{M^2} = \frac{N_{\rm c}\alpha^3}{8\pi}\lim_{\delta\to 0}\int_{\delta}^{\infty}{\rm d}\varrho\;{\rm Im}\biggl\{\frac{1}{[g^0_{\rm r}(\varrho)]^2}\biggr\}\biggr|_{g^0_{\rm r}(\varrho)=\varrho-\varrho^2/2+\ldots}\;. \tag{A.23}$$

In other words, comparing with eq. (4.25), $\delta_0\rho^S(\omega') = -\alpha^2\rho^V(\omega')/12$; the factor α^2 is a manifestation of the suppression $\sim \nabla^2_{\mathbf{r}}/M^2$ apparent in eq. (3.30), combined with the parametric order of magnitude of $\nabla_{\mathbf{r}}/M$ from eq. (3.1).

Consider then the contribution from the mode $l = 1$ (P-wave). The relevant term from eq. (4.22), denoted by $\delta_1\tilde{\Psi}$, is

$$\delta_1\tilde{\Psi}(\omega';\mathbf{r},\mathbf{r}') = A\frac{g^1_<(r)}{r}\frac{g^1_>(r')}{r'}\sum_{m=-1}^{1}Y_{1m}(\theta,\phi)Y^*_{1m}(\theta',\phi')\;. \tag{A.24}$$

Hence we will need

$$Y_{10}(\theta,\phi) = \sqrt{\frac{3}{4\pi}}\cos\theta\;,\quad Y_{1\pm1}(\theta,\phi) = \mp\sqrt{\frac{3}{8\pi}}\sin\theta e^{\pm i\phi}\;. \tag{A.25}$$

In order to take the derivatives in eq. (4.16), we stay with radial coordinates, so that

$$\nabla_{\mathbf{r}} = \mathbf{e}_r \frac{\partial}{\partial r} + \mathbf{e}_\theta \frac{1}{r}\frac{\partial}{\partial \theta} + \mathbf{e}_\phi \frac{1}{r\sin\theta}\frac{\partial}{\partial \phi} \,. \tag{A.26}$$

Moreover, we choose again $r < r'$, so that $r_< \equiv r$, $r_> \equiv r'$. We will set $\Omega' = \Omega$ after taking the derivatives in eq. (4.16), so that the basis is orthogonal. Making use of eqs. (A.26), (A.25), the terms $m = \pm 1$ both yield

$$\nabla_{\mathbf{r}'} \cdot \nabla_{\mathbf{r}}\, \delta_1\tilde{\Psi} = A\frac{3}{8\pi}\left\{ \frac{\partial}{\partial r}\left[\frac{g^1_<(r)}{r}\right]\frac{\partial}{\partial r'}\left[\frac{g^1_>(r')}{r'}\right]\sin^2\theta + \frac{g^1_<(r)}{r^2}\frac{g^1_>(r')}{(r')^2}\left[\cos^2\theta + 1\right]\right\}, \tag{A.27}$$

while the term $m = 0$ yields

$$\nabla_{\mathbf{r}'} \cdot \nabla_{\mathbf{r}}\, \delta_1\tilde{\Psi} = A\frac{3}{4\pi}\left\{ \frac{\partial}{\partial r}\left[\frac{g^1_<(r)}{r}\right]\frac{\partial}{\partial r'}\left[\frac{g^1_>(r')}{r'}\right]\cos^2\theta + \frac{g^1_<(r)}{r^2}\frac{g^1_>(r')}{(r')^2}\sin^2\theta\right\}. \tag{A.28}$$

Summing together, we get

$$\nabla_{\mathbf{r}'} \cdot \nabla_{\mathbf{r}}\, \delta_1\tilde{\Psi} = A\frac{3}{4\pi}\left\{ \frac{\partial}{\partial r}\left[\frac{g^1_<(r)}{r}\right]\frac{\partial}{\partial r'}\left[\frac{g^1_>(r')}{r'}\right] + 2\frac{g^1_<(r)}{r^2}\frac{g^1_>(r')}{(r')^2}\right\}. \tag{A.29}$$

We now insert $g^1_<(r) = g^1_{\rm r}(r)$, $g^1_>(r') = -g^1_{\rm r}(r')\int_{r'}^\infty {\rm d}r''\, 1/[g^1_{\rm r}(r'')]^2$ from eqs. (A.3), (A.6), and recall that at small r, $g^1_{\rm r}(r) \approx \varrho^2 = (r\alpha M)^2$. Thereby

$$\lim_{\mathbf{r},\mathbf{r}'\to\mathbf{0}} \nabla_{\mathbf{r}'}\cdot\nabla_{\mathbf{r}}\, \delta_1\tilde{\Psi} = -\frac{3A}{4\pi}(\alpha M)^3 \lim_{\varrho'\to 0}\left\{ \frac{\mathrm{d}}{\mathrm{d}\varrho'}\left(\frac{g^1_{\rm r}(\varrho')}{\varrho'}\int_{\varrho'}^\infty \frac{\mathrm{d}\varrho''}{[g^1_{\rm r}(\varrho'')]^2}\right) + \frac{2g^1_{\rm r}(\varrho')}{(\varrho')^2}\int_{\varrho'}^\infty \frac{\mathrm{d}\varrho''}{[g^1_{\rm r}(\varrho'')]^2}\right\}. \tag{A.30}$$

Inserting this into eq. (4.16), and making use of eq. (A.8), we get

$$\frac{\delta_1\rho^S(\omega')}{M^2} = \frac{3N_{\rm c}}{2\pi}\alpha^3 \lim_{\varrho'\to 0}{\rm Im}\left\{\left[\frac{\mathrm{d}}{\mathrm{d}\varrho'}\left(\frac{g^1_{\rm r}(\varrho')}{\varrho'}\right) + \frac{2g^1_{\rm r}(\varrho')}{(\varrho')^2}\right]\int_{\varrho'}^\infty \frac{\mathrm{d}\varrho''}{[g^1_{\rm r}(\varrho'')]^2} - \frac{1}{\varrho' g^1_{\rm r}(\varrho')}\right\}. \tag{A.31}$$

Once again, we need to inspect the origin of the imaginary part. According to eqs. (A.11), (A.13), ${\rm Re}[g^1_{\rm r}(\varrho')] \sim (\rho')^2$, ${\rm Im}[g^1_{\rm r}(\varrho')] \sim (\rho')^6$, and consequently

$${\rm Re}\left\{\frac{1}{[g^1_{\rm r}(\varrho'')]^2}\right\} \approx \frac{1}{(\varrho'')^4}\,, \quad {\rm Im}\left\{\frac{1}{\varrho' g^1_{\rm r}(\varrho')}\right\} \approx {\rm Im}\left\{\frac{1}{(\varrho')^3 + i\gamma_1(\varrho')^7}\right\} \approx -\gamma_1\varrho'\,, \tag{A.32}$$

so that the only possibility is to consider ${\rm Im}\{1/[g^1_{\rm r}(\varrho'')]^2\}$. The prefactor multiplying this can be trivially determined, and we end up with

$$\frac{\delta_1\rho^S(\omega')}{M^2} = \frac{9N_{\rm c}}{2\pi}\alpha^3 \lim_{\delta\to 0}\int_\delta^\infty {\rm d}\varrho\ {\rm Im}\left\{\frac{1}{[g^1_{\rm r}(\varrho)]^2}\right\}\Bigg|_{g^1_{\rm r}(\varrho)=\varrho^2-\varrho^3/4+\ldots}, \tag{A.33}$$

in analogy with eq. (4.25). Combining eqs. (A.23), (A.33), the complete scalar channel spectral function can be written as in eq. (4.26).

To conclude, let us again check that the procedure introduced does yield the correct tree-level result. Somewhat unfortunately, the first term in eq. (4.26) does not contribute in this limit: the subleading term in eq. (A.11) would be of $\mathcal{O}(\varrho^{l+3})$ in the free case, so

that $g^0_{\rm r}/\varrho \sim \varrho^2$ in eq. (A.20), and $\delta_0\rho^S$ vanishes. However, the second term in eq. (4.26) survives. In dimensionless variables, the homogeneous Schrödinger equation reads

$$\left[\frac{\mathrm{d}^2}{\mathrm{d}\varrho^2} - \frac{2}{\varrho^2} + \frac{\hat{\omega}'}{\alpha^2} + i\epsilon\right] g^1_{\rm r}(\varrho) = 0\,. \tag{A.34}$$

Since there is no imaginary potential, we have had to introduce $\epsilon \equiv 0^+$ to pick up the retarded solution. The solution normalised to give the desired small-ϱ behaviour [$g^1_{\rm r}(\varrho) = \varrho^2 + \ldots$] is

$$g^1_{\rm r}(\varrho) = \frac{3}{k^2}\left[\frac{\sin(k\varrho)}{k\varrho} - \cos(k\varrho)\right], \tag{A.35}$$

where k is from eq. (A.15). We note that

$$\left[\frac{\sin(k\varrho)}{k\varrho} - \cos(k\varrho)\right]^{-2} = \frac{1}{k}\frac{\mathrm{d}}{\mathrm{d}\varrho}\left[\frac{\cos(k\varrho) + k\varrho\sin(k\varrho)}{k\varrho\cos(k\varrho) - \sin(k\varrho)}\right], \tag{A.36}$$

whereby

$$\begin{aligned}\frac{\rho^S(\omega')}{M^2} &= \frac{9N_{\rm c}}{2\pi}\alpha^3 \lim_{\varrho\to\infty} \mathrm{Im}\left\{\frac{1}{9}\left(\frac{\hat{\omega}'}{\alpha^2} + i\epsilon\right)^{\frac{3}{2}} \frac{\cos(k\varrho) + k\varrho\sin(k\varrho)}{k\varrho\cos(k\varrho) - \sin(k\varrho)}\right\} \\ &= \frac{N_{\rm c}}{2\pi}\alpha^3\,\mathrm{Im}\left\{\left(\frac{\hat{\omega}'}{\alpha^2} + i\epsilon\right)^{\frac{3}{2}} i\right\} = \frac{N_{\rm c}}{2\pi}\,\theta(\omega')\,(\hat{\omega}')^{\frac{3}{2}}\,.\end{aligned} \tag{A.37}$$

This indeed agrees with eq. (3.36).

References

[1] NA50 collaboration, B. Alessandro et al., *A new measurement of J/ψ suppression in Pb-Pb collisions at 158-GeV per nucleon*, *Eur. Phys. J.* **C 39** (2005) 335 [hep-ex/0412036];
PHENIX collaboration, A. Adare et al., *J/ψ production vs centrality, transverse momentum and rapidity in $Au + Au$ collisions at $\sqrt{s_{NN}} = 200$ GeV*, *Phys. Rev. Lett.* **98** (2007) 232301 [nucl-ex/0611020];
NA60 collaboration, R. Arnaldi et al., *J/ψ suppression in In-In collisions at 158 GeV/nucleon*, *Nucl. Phys.* **A 783** (2007) 261 [nucl-ex/0701033].

[2] T. Matsui and H. Satz, *J/ψ suppression by quark-gluon plasma formation*, *Phys. Lett.* **B 178** (1986) 416;
H. Satz, *Colour deconfinement and quarkonium binding*, *J. Phys.* **G 32** (2006) R25 [hep-ph/0512217].

[3] Quarkonium Working Group collaboration, N. Brambilla et al., *Heavy quarkonium physics*, hep-ph/0412158.

[4] T. Umeda, K. Nomura and H. Matsufuru, *Charmonium at finite temperature in quenched lattice QCD*, *Eur. Phys. J.* **C 39S1** (2005) 9 [hep-lat/0211003];
M. Asakawa and T. Hatsuda, *J/ψ and η_c in the deconfined plasma from lattice QCD*, *Phys. Rev. Lett.* **92** (2004) 012001 [hep-lat/0308034];
S. Datta, F. Karsch, P. Petreczky and I. Wetzorke, *Behavior of charmonium systems after deconfinement*, *Phys. Rev.* **D 69** (2004) 094507 [hep-lat/0312037];
H. Iida, T. Doi, N. Ishii, H. Suganuma and K. Tsumura, *Charmonium properties in deconfinement phase in anisotropic lattice QCD*, *Phys. Rev.* **D 74** (2006) 074502 [hep-lat/0602008].

JHEP01(2008)043

[5] A. Jakovác, P. Petreczky, K. Petrov and A. Velytsky, *Quarkonium correlators and spectral functions at zero and finite temperature*, *Phys. Rev.* **D 75** (2007) 014506 [hep-lat/0611017].

[6] G. Aarts, C. Allton, M.B. Oktay, M. Peardon and J.I. Skullerud, *Charmonium at high temperature in two-flavor QCD*, *Phys. Rev.* **D 76** (2007) 094513 [arXiv:0705.2198].

[7] S. Digal, P. Petreczky and H. Satz, *String breaking and quarkonium dissociation at finite temperatures*, *Phys. Lett.* **B 514** (2001) 57 [hep-ph/0105234];
C.Y. Wong, *Heavy quarkonia in quark gluon plasma*, *Phys. Rev.* **C 72** (2005) 034906 [hep-ph/0408020];
F. Arleo, J. Cugnon and Y. Kalinovsky, *Heavy-quarkonium interaction in QCD at finite temperature*, *Phys. Lett.* **B 614** (2005) 44 [hep-ph/0410295];
D. Cabrera and R. Rapp, *T-matrix approach to quarkonium correlation functions in the QGP*, *Phys. Rev.* **D 76** (2007) 114506 [hep-ph/0611134];
W.M. Alberico, A. Beraudo, A. De Pace and A. Molinari, *Potential models and lattice correlators for quarkonia at finite temperature*, arXiv:0706.2846.

[8] A. Mócsy and P. Petreczky, *Can quarkonia survive deconfinement?*, arXiv:0705.2559.

[9] O. Jahn and O. Philipsen, *The Polyakov loop and its relation to static quark potentials and free energies*, *Phys. Rev.* **D 70** (2004) 074504 [hep-lat/0407042].

[10] O. Kaczmarek and F. Zantow, *Static quark anti-quark interactions at zero and finite temperature QCD. II: quark anti-quark internal energy and entropy*, hep-lat/0506019;
WHOT-QCD collaboration, Y. Maezawa et al., *Heavy-quark free energy, Debye mass and spatial string tension at finite temperature in two flavor lattice QCD with Wilson quark action*, *Phys. Rev.* **D 75** (2007) 074501 [hep-lat/0702004];
M. Döring, K. Hübner, O. Kaczmarek and F. Karsch, *Color screening and quark-quark interactions in finite temperature QCD*, *Phys. Rev.* **D 75** (2007) 054504 [hep-lat/0702009].

[11] K. Peeters, J. Sonnenschein and M. Zamaklar, *Holographic melting and related properties of mesons in a quark gluon plasma*, *Phys. Rev.* **D 74** (2006) 106008 [hep-th/0606195];
H. Liu, K. Rajagopal and U.A. Wiedemann, *An AdS/CFT calculation of screening in a hot wind*, *Phys. Rev. Lett.* **98** (2007) 182301 [hep-ph/0607062];
M. Chernicoff, J.A. García and A. Güijosa, *The energy of a moving quark-antiquark pair in an $\mathcal{N} = 4$ SYM plasma*, *JHEP* **09** (2006) 068 [hep-th/0607089];
E. Cáceres, M. Natsuume and T. Okamura, *Screening length in plasma winds*, *JHEP* **10** (2006) 011 [hep-th/0607233];
S.D. Avramis, K. Sfetsos and D. Zoakos, *On the velocity and chemical-potential dependence of the heavy-quark interaction in $\mathcal{N} = 4$ SYM plasmas*, *Phys. Rev.* **D 75** (2007) 025009 [hep-th/0609079];
C. Hoyos, K. Landsteiner and S. Montero, *Holographic meson melting*, *JHEP* **04** (2007) 031 [hep-th/0612169];
R.C. Myers, A.O. Starinets and R.M. Thomson, *Holographic spectral functions and diffusion constants for fundamental matter*, *JHEP* **11** (2007) 091 [arXiv:0706.0162].

[12] M. Laine and Y. Schröder, *Two-loop QCD gauge coupling at high temperatures*, *JHEP* **03** (2005) 067 [hep-ph/0503061].

[13] P.H. Ginsparg, *First order and second order phase transitions in gauge theories at finite temperature*, *Nucl. Phys.* **B 170** (1980) 388;
T. Appelquist and R.D. Pisarski, *High-temperature Yang-Mills theories and three-dimensional quantum chromodynamics*, *Phys. Rev.* **D 23** (1981) 2305;

JHEP01(2008)043

K. Kajantie, M. Laine, K. Rummukainen and M.E. Shaposhnikov, *Generic rules for high temperature dimensional reduction and their application to the standard model*, *Nucl. Phys.* **B 458** (1996) 90 [hep-ph/9508379].

[14] R.D. Pisarski, *Scattering amplitudes in hot gauge theories*, *Phys. Rev. Lett.* **63** (1989) 1129;
J. Frenkel and J.C. Taylor, *High temperature limit of thermal QCD*, *Nucl. Phys.* **B 334** (1990) 199;
E. Braaten and R.D. Pisarski, *Soft amplitudes in hot gauge theories: a general analysis*, *Nucl. Phys.* **B 337** (1990) 569;
J.C. Taylor and S.M.H. Wong, *The effective action of hard thermal loops in QCD*, *Nucl. Phys.* **B 346** (1990) 115.

[15] J.I. Kapusta, *Quantum chromodynamics at high temperature*, *Nucl. Phys.* **B 148** (1979) 461;
C. Zhai and B.M. Kastening, *The free energy of hot gauge theories with fermions through g^5*, *Phys. Rev.* **D 52** (1995) 7232 [hep-ph/9507380];
A. Vuorinen, *Quark number susceptibilities of hot QCD up to $g^6 ln(g)$*, *Phys. Rev.* **D 67** (2003) 074032 [hep-ph/0212283].

[16] S. Caron-Huot and G.D. Moore, *Heavy quark diffusion in perturbative QCD at next-to-leading order*, arXiv:0708.4232.

[17] T. Toimela, *The next term in the thermodynamic potential of QCD*, *Phys. Lett.* **B 124** (1983) 407;
P. Arnold and C. Zhai, *The three loop free energy for pure gauge QCD*, *Phys. Rev.* **D 50** (1994) 7603 [hep-ph/9408276]; *The three loop free energy for high temperature QED and QCD with fermions*, *Phys. Rev.* **D 51** (1995) 1906 [hep-ph/9410360];
K. Kajantie, M. Laine, K. Rummukainen and Y. Schröder, *The pressure of hot QCD up to $g^6 ln(1/g)$*, *Phys. Rev.* **D 67** (2003) 105008 [hep-ph/0211321].

[18] A.K. Rebhan, *The nonabelian Debye mass at next-to-leading order*, *Phys. Rev.* **D 48** (1993) 3967 [hep-ph/9308232].

[19] A.D. Linde, *Infrared problem in thermodynamics of the Yang-Mills gas*, *Phys. Lett.* **B 96** (1980) 289;
D.J. Gross, R.D. Pisarski and L.G. Yaffe, *QCD and instantons at finite temperature*, *Rev. Mod. Phys.* **53** (1981) 43.

[20] P. Arnold and L.G. Yaffe, *The nonabelian Debye screening length beyond leading order*, *Phys. Rev.* **D 52** (1995) 7208 [hep-ph/9508280];
M. Laine and O. Philipsen, *The non-perturbative QCD Debye mass from a Wilson line operator*, *Phys. Lett.* **B 459** (1999) 259 [hep-lat/9905004].

[21] A. Hietanen, K. Kajantie, M. Laine, K. Rummukainen and Y. Schröder, *Plaquette expectation value and gluon condensate in three dimensions*, *JHEP* **01** (2005) 013 [hep-lat/0412008];
A. Hietanen and A. Kurkela, *Plaquette expectation value and lattice free energy of three-dimensional* SU(N_c) *gauge theory*, *JHEP* **11** (2006) 060 [hep-lat/0609015];
F. Di Renzo, M. Laine, V. Miccio, Y. Schröder and C. Torrero, *The leading non-perturbative coefficient in the weak-coupling expansion of hot QCD pressure*, *JHEP* **07** (2006) 026 [hep-ph/0605042].

[22] E. Braaten and A. Nieto, *Free energy of QCD at high temperature*, *Phys. Rev.* **D 53** (1996) 3421 [hep-ph/9510408].

JHEP01(2008)043

[23] J.P. Blaizot, E. Iancu and A. Rebhan, *On the apparent convergence of perturbative QCD at high temperature*, *Phys. Rev.* **D 68** (2003) 025011 [hep-ph/0303045];
M. Laine and M. Vepsäläinen, *Mesonic correlation lengths in high-temperature QCD*, *JHEP* **02** (2004) 004 [hep-ph/0311268];
P. Giovannangeli, *Two loop renormalization of the magnetic coupling and non- perturbative sector in hot QCD*, *Nucl. Phys.* **B 738** (2006) 23 [hep-ph/0506318].

[24] M. Laine, O. Philipsen, P. Romatschke and M. Tassler, *Real-time static potential in hot QCD*, *JHEP* **03** (2007) 054 [hep-ph/0611300].

[25] M. Laine, *A resummed perturbative estimate for the quarkonium spectral function in hot QCD*, *JHEP* **05** (2007) 028 [arXiv:0704.1720].

[26] M. Laine, O. Philipsen and M. Tassler, *Thermal imaginary part of a real-time static potential from classical lattice gauge theory simulations*, *JHEP* **09** (2007) 066 [arXiv:0707.2458].

[27] L.D. McLerran and T. Toimela, *Photon and dilepton emission from the quark-gluon plasma: some general considerations*, *Phys. Rev.* **D 31** (1985) 545;
H.A. Weldon, *Reformulation of finite temperature dilepton production*, *Phys. Rev.* **D 42** (1990) 2384;
C. Gale and J.I. Kapusta, *Vector dominance model at finite temperature*, *Nucl. Phys.* **B 357** (1991) 65.

[28] A. Pineda and J. Soto, *Effective field theory for ultrasoft momenta in NRQCD and NRQED*, *Nucl. Phys.* **64** *(Proc. Suppl.)* (1998) 428 [hep-ph/9707481];
N. Brambilla, A. Pineda, J. Soto and A. Vairo, *Potential NRQCD: an effective theory for heavy quarkonium*, *Nucl. Phys.* **B 566** (2000) 275 [hep-ph/9907240].

[29] W.E. Caswell and G.P. Lepage, *Effective lagrangians for bound state problems in QED, QCD and other field theories*, *Phys. Lett.* **B 167** (1986) 437.

[30] N. Brambilla, A. Pineda, J. Soto and A. Vairo, *Effective field theories for heavy quarkonium*, *Rev. Mod. Phys.* **77** (2005) 1423 [hep-ph/0410047].

[31] J.G. Körner and G. Thompson, *The heavy mass limit in field theory and the heavy quark effective theory*, *Phys. Lett.* **B 264** (1991) 185.

[32] K.G. Chetyrkin and M. Steinhauser, *Short distance mass of a heavy quark at order α_s^3*, *Phys. Rev. Lett.* **83** (1999) 4001 [hep-ph/9907509].

[33] A. Czarnecki and K. Melnikov, *Two-loop QCD corrections to the heavy quark pair production cross section in e^+e^- annihilation near the threshold*, *Phys. Rev. Lett.* **80** (1998) 2531 [hep-ph/9712222];
M. Beneke, A. Signer and V.A. Smirnov, *Two-loop correction to the leptonic decay of quarkonium*, *Phys. Rev. Lett.* **80** (1998) 2535 [hep-ph/9712302].

[34] T. Umeda, R. Katayama, O. Miyamura and H. Matsufuru, *Study of charmonia near the deconfining transition on an anisotropic lattice with $O(a)$ improved quark action*, *Int. J. Mod. Phys.* **A 16** (2001) 2215 [hep-lat/0011085].

[35] T. Hatsuda, *Bulk and spectral observables in lattice QCD*, *J. Phys.* **G 34** (2007) S287 [hep-ph/0702293].

[36] M.J. Strassler and M.E. Peskin, *The heavy top quark threshold: QCD and the Higgs*, *Phys. Rev.* **D 43** (1991) 1500.

JHEP01(2008)043

[37] K. Kajantie, M. Laine, K. Rummukainen and M.E. Shaposhnikov, $3D$ SU(N) + *adjoint Higgs theory and finite-temperature QCD*, *Nucl. Phys.* **B 503** (1997) 357 [hep-ph/9704416].

[38] F. Karsch, E. Laermann, P. Petreczky and S. Stickan, *Infinite temperature limit of meson spectral functions calculated on the lattice*, *Phys. Rev.* **D 68** (2003) 014504 [hep-lat/0303017];
G. Aarts and J.M. Martínez Resco, *Continuum and lattice meson spectral functions at nonzero momentum and high temperature*, *Nucl. Phys.* **B 726** (2005) 93 [hep-lat/0507004];
A. Mócsy and P. Petreczky, *Quarkonia correlators above deconfinement*, *Phys. Rev.* **D 73** (2006) 074007 [hep-ph/0512156];
UKQCD collaboration, G. Aarts and J. Foley, *Meson spectral functions with chirally symmetric lattice fermions*, *JHEP* **02** (2007) 062 [hep-lat/0612007].

[39] M. Beneke, *Perturbative heavy quark-antiquark systems*, hep-ph/9911490.

[40] G. Aarts, C. Allton, J. Foley, S. Hands and S. Kim, *Spectral functions at small energies and the electrical conductivity in hot, quenched lattice QCD*, *Phys. Rev. Lett.* **99** (2007) 022002 [hep-lat/0703008];
H.B. Meyer, *A calculation of the shear viscosity in* SU(3) *gluodynamics*, *Phys. Rev.* **D 76** (2007) 101701 [arXiv:0704.1801].

JHEP01(2008)043